Salmonella Typhimurium outer membrane protein A (OmpA) renders protection against nitrosative stress by promoting SCV stability in murine macrophages

Atish Roy Chowdhury[1, 2], Shivjee Sah[1, 2], Umesh Varshney[1, 2] and Dipshikha Chakravortty[1, 2, 3*]

[1]Department of Microbiology and Cell Biology, Indian Institute of Science, Bangalore, Karnataka, India-560012

[2]Division of Biological Sciences, Indian Institute of Science, Bangalore, Karnataka, India-560012

[3]Centre for Biosystems Science and Engineering, Indian Institute of Science, Bangalore, Karnataka, India-560012.

Current address: Department of Microbiology and Cell Biology, Indian Institute of Science, Bangalore, Karnataka, India-560012

* *Corresponding author*

Dipshikha Chakravortty

Email: dipa@ iisc.ac.in

Tel: 0091 80 2293 2842

Fax: 0091 80 2360 2697

23

Abstract

Porins are highly conserved bacterial outer membrane proteins involved in the selective transport of charged molecules across the membrane. Despite their important contributions to the pathogenesis of Gram-negative bacteria, their precise role in salmonellosis remains elusive. In this study, we investigated the role of porins (OmpA, OmpC, OmpD, and OmpF) in *Salmonella* Typhimurium (STM) pathogenesis. OmpA played a multifaceted role in STM pathogenesis, and a strain deleted for *ompA* (STM *ΔompA*) showed enhanced proneness to phagocytosis and compromised proliferation in macrophages. However, in epithelial cells, despite being invasion deficient, it was hyper-proliferative. The poor colocalization of STM *ΔompA* with LAMP-1 confirmed impaired stability of SCV membrane around the intracellular bacteria, resulting in its (STM *ΔompA*) release into the cytosol of macrophages where it is assaulted with reactive nitrogen intermediates (RNI). The cytosolic localization of STM *ΔompA* was responsible for the downregulation of SPI-2 encoded virulence factor SpiC, which is required to suppress the activity of iNOS. The reduced recruitment of nitrotyrosine on STM in the macrophage cytosol upon ectopically expressing Listeriolysin O (LLO) explicitly supported the pro-bacterial role of OmpA against the host nitrosative stress. Further, we show that time-dependent generation of redox burst could be responsible for the enhanced sensitivity of STM *ΔompA* towards nitrosative stress. The absence of OmpA in STM *ΔompA* resulted in the loss of integrity and enhanced porosity of the outer membrane, which was attributed to the upregulated expression of *ompC*, *ompD*, and *ompF*. We show the involvement of OmpC and OmpF in the entry of excess nitrite in STM *ΔompA*. In conclusion, we illustrated a mechanism of strategic utilization of OmpA compared to other porins by wildtype *Salmonella* for combating the nitrosative stress in macrophages.

Keywords: *Salmonella* Typhimurium, Outer membrane protein A, *Salmonella* containing vacuole, Nitrosative stress, Reactive Nitrogen Intermediates, Outer membrane protein C, Outer membrane protein D, Outer membrane protein F.

Introduction

Salmonella enterica Serovar Typhimurium is a Gram-negative, rod-shaped, flagellated, facultative anaerobic bacterium belonging to the family *Enterobacteriaceae* and a principal causative agent of typhoid fever-like symptoms in mice and self-limiting gastroenteritis in humans (Haraga et al., 2008, Galan, 2001). If not treated in time, typhoid fever is fatal and poses a severe threat to global health. Despite a significant reduction in the incidence and fatality in the past two decades, typhoid fever remains a major cause of morbidity and mortality in developing nations. Globally, the occurrence of ~14.3 million cases with ~135.9 thousand deaths due to typhoid and paratyphoid fever was registered in 2017 (Collaborators, 2019). *Salmonella* Typhimurium rapidly spreads through the contaminated food and water when ingested by healthy individuals. After entering the host's body, Salmonella eventually adheres and invades the small intestine's epithelial cells and crosses the mucosal barrier through the M cells (microfold cells) of Peyer's patches. During the systemic phase of infection, wildtype *Salmonella* inhabiting macrophages, dendritic cells, or polymorphonuclear cells can reach many parts of the body, namely the liver, spleen, mesenteric lymph node (MLN), brain, bone marrow, gall bladder, etc. (Gogoi et al., 2019). The infection caused by *Salmonella* is predominantly governed by two extensively characterized pathogenicity islands called SPI-1 and SPI-2 coding for a plethora of effector proteins and two distinct type 3 secretion systems (T3SS), which broadly regulate the adhesion, invasion, and intracellular survival of the bacteria (Garai et al., 2012).

The pathogenicity of many Gram-negative bacteria of the family *Enterobacteriaceae* is regulated by porins, commonly known as outer membrane proteins (or Omp). Porins are outer membrane-bound β barrel proteins with 8 to 24 antiparallel β strands connected by loops and are well known for their role in the selective diffusion of ions and solutes across the outer membrane of bacteria (Vergalli et al., 2020). Despite their roles in maintaining outer membrane stability, their pathogenic functions have also been well documented. OmpA, one of the most abundant porins of the bacterial outer membrane, is extensively utilized by *Klebsiella pneumoniae* to prevent the IL-8 dependent pro-inflammatory response in the airway epithelial A549 cells (March et al., 2011). The deletion of *ompC* and *ompF* from pathogenic *E. coli* not only impaired its invasion in bEnd.3 cells but also reduced its virulence in a mouse model (Hejair et al., 2017). OprF, an OmpA ortholog in the outer membrane of *Pseudomonas sp.* has been reported to function as a quorum signaling sensor and induce virulence (Krishnan and Prasadarao, 2012). OmpW of *E. coli* has been reported to play a significant role against phagocytosis and complement activation (Wu et al., 2013, Li et al., 2016).

The outer membrane of *Salmonella* Typhimurium, a member of the *Enterobacteriaceae* family, is densely populated with many porins such as OmpA, OmpC, OmpD, and OmpF. Unlike OmpA, which has a significant role in the tight attachment of the outer membrane to the underlying peptidoglycan layer with its periplasmic tail (Park et al., 2012), the other porins facilitate transportation of charged ions (Ipinza et al., 2014). The connection between the outer membrane porins of *Salmonella* Typhimurium and its pathogenesis remains elusive due to the lack of detailed studies. Earlier, Heijden *et al*. proposed a mechanism of OmpA and OmpC dependent regulation of outer membrane permeability in *Salmonella* in response to H_2O_2 and antibiotic stresses (Heijden et al., 2016).

In the current study, we have investigated the individual roles of OmpA, OmpC, OmpD, and OmpF in the pathogenesis of *Salmonella* Typhimurium with a critical focus on OmpA. We

found a strong dependence of *Salmonella* on OmpA for its survival in macrophages and the mouse model. Our study illustrates a mechanism of strategic utilization of OmpA, compared with other porins, by *Salmonella* in combating macrophages' nitrosative stress and endorse the importance of OmpA in the regulation of outer membrane stability. To the best of our knowledge, this is the first study to demonstrate the impact of outer membrane porins in the maintenance of vacuolar stability of *Salmonella* in macrophages and the epithelial cells.

Results

OmpA promotes the evasion of phagocytosis and intracellular survival of *Salmonella* in macrophages.

The transcriptomic analyses of intracellular *Salmonella* Typhimurium infecting J774-A.1 and HeLa cells have demonstrated almost 2 to 2.5 fold induction in the expression level of *ompA* during early (4h), middle (8h), and late (12h) stages of infection in comparison with other major membrane porins namely *ompC*, *ompD*, and *ompF* (Eriksson et al., 2003), (Hautefort et al., 2008). To validate this observation, we isolated total RNA from *Salmonella* Typhimurium strain 14028S grown in nutritionally enriched Luria-Bertani broth, low magnesium minimal acidic F media (pH= 5.4) mimicking the nutrient-deprived acidic environment of *Salmonella* containing vacuole (SCV) (Deiwick et al., 1999), and RAW264.7 cells at different time points (3, 6, 9, 12 h post-inoculation/ infection) and investigated the transcript levels of *ompA* (Figure S1A), *ompC* (Figure S1B), *ompD* (Figure S1C), and *ompF* (Figure S1D) by real-time PCR. Unlike the steady decrease in the expression levels of *ompC*, *ompD*, and *ompF*, whose expression steadily decreased in wild type bacteria growing in LB broth, F media, and macrophage at all the time points except for *ompF* in macrophage at 9th h post-infection, there was a significant increase in the transcript level of *ompA* during the late phase of infection (9h and 12 h post-infection) in macrophage (Figure S1A, S1D). These observations suggest a

strong preference of *ompA* over the other membrane-bound larger porins to enable *Salmonella* to thrive inside macrophages. The observation is also consistent with the microarray data published by Eriksson *et al*. and Hautefort *et al.* (Eriksson et al., 2003, Hautefort et al., 2008). To investigate the importance of *ompA* in the intracellular survival of *Salmonella*, we knocked out *ompA* from the genome of *Salmonella* Typhimurium (Figure S2A and S2B) (Datsenko and Wanner, 2000). The *ompA* gene (1.3 kb) was replaced with a kanamycin-resistant cassette (1.7 kb) (Figure S2A). The knockout was further confirmed with kanamycin-resistant gene cassette-specific internal primers (amplicon of 0.47 kb) (Figure S2B). Complementation of the strain with a plasmid (cloned in pQE60) borne *ompA* resulted in ~1.42-fold overexpression of *ompA* compared to the wild type *S.* Typhimurium] (Figure S2D). It was also found that knocking out of *ompA* from *Salmonella* did not alter the *in vitro* growth of the bacteria in LB broth (Figure S2E and S2F). To determine the role of *S.* Typhimurium *ompA* in phagocytosis, we checked phagocytosis of the wild type and knockout strains in macrophages (Figure 1A). We found that OmpA of STM helps it to evade phagocytosis by RAW264.7 and activated U937 cells (Figure 1A). The percent phagocytosis of STM *ΔompA* in RAW 264.7 and U937 cells is more than STM (wild type, WT). The complemented strain is less prone to phagocytosis by the macrophage-like wild-type *S.* Typhimurium in both the cell lines. Adhesion of bacteria onto the host cell surface occurs before entering into the host cell, either by phagocytosis or by invasion (Garai et al., 2016). Since we found enhanced phagocytosis of STM *ΔompA* in macrophages compared to wild-type bacteria, we decided to evaluate the bacterial attachment on macrophage surface by *in vitro* adhesion assay (Figure 1B). The adhesion of STM *ΔompA* on phagocytic RAW 264.7 cells is more compared to STM (WT) (Figure 1B). The enhanced adhesion of STM *ΔompA* was abrogated upon complementation with *ompA*. We then performed the intracellular survival assay of STM (WT) and STM *ΔompA* strains in RAW264.7, activated U937 cells respectively (Figure 1C). We observed that the intracellular growth of STM *ΔompA*

144 [fold proliferation in RAW264.7 cells- 11.45± 3.349, U937 cells- 5.075± 1.157] is significantly
145 attenuated in RAW 264.7 (Figure 1I) (by 2.75 folds) and activated U937 (Figure 1J) cells (by
146 3.08 folds) compared to the wild type parent [fold proliferation in RAW264.7 cells- 31.5±
147 5.347, U937 cells- 15.65± 3.981]. When the cell lines were infected with the complemented
148 strain, there was a recovery of the intracellular proliferation of bacteria (Figure 1C). Hence, we
149 conclude that *Salmonella* utilizes OmpA as a double-edged sword to protect the bacteria from
150 phagocytosis and then for its survival in macrophages. Once ingested, *Salmonella* starts
151 invading M cells of the Payer's patch in the small intestine with the help of SPI-1 encoded type
152 3 secretion system. Hence, we checked the role of *Salmonella* OmpA in bacterial invasion of
153 non-phagocytic epithelial cells (Figure S3A). In comparison with the wild-type bacteria, STM
154 *ΔompA* exhibited notable attenuation in the invasion of human colorectal adenocarcinoma cell
155 line- Caco-2 and human cervical cancer cell line- HeLa (Figure S3A), and the invasiveness was
156 rescued upon complementation (Figure S3A). To validate this observation further, we carried
157 out *in vitro* adhesion assay using HeLa cells as host (Figure S3B). STM *ΔompA* showed reduced
158 attachment on the surface of HeLa cells compared to the wild-type bacteria (Figure S3B). The
159 inefficiency of the knockout strain to attach to the epithelial cell surface was rescued in the
160 complemented strain (Figure S3B). This observation is consistent with the result obtained from
161 the invasion assay and showed utilization OmpA by *Salmonella* as an adhesion and invasion
162 tool is of paramount importance. We further verified the role of OmpA in the maintenance of
163 intracellular life of bacteria in epithelial cells (Figure S3C). Surprisingly, STM *ΔompA*
164 exhibited hyperproliferation in both Caco-2 and HeLa cells (Figure S3C) compared to wild-
165 type bacteria. The intracellular proliferation of complement strain was comparable to the wild-
166 type bacteria in both the cell lines. Since we found opposite outcomes in the intracellular
167 survival of the *ompA* knockout strain of *Salmonella* in two different cell types (attenuation in
168 macrophage and hyper-proliferation in the epithelial cell), we decided to monitor the

169 intracellular niche of the bacteria in both cell types. After entering the host cells, *Salmonella*
170 resides inside a modified phagosomal compartment called *Salmonella* Containing Vacuole
171 (SCV), which is acidic. The intracellular life and proliferation of *Salmonella* depend upon the
172 stability and integrity of SCV. *Salmonella* recruits a plethora of host proteins to maintain the
173 sustainability of SCV. During the early stage of infection in macrophage and epithelial cells,
174 SCV is characterized by the presence of markers of early endocytic pathway such as EEA1,
175 Rab5, Rab4, Rab11 and transferrin receptors, etc. These proteins are replaced by the markers
176 of late endosome such as LAMP-1, Rab7, vATPase etc within 15 to 45 min post infection
177 (Garai et al., 2012, Knuff and Finlay, 2017). Since we found an attenuation in the intracellular
178 proliferation of STM *ΔompA* in macrophage and hyperproliferation in epithelial cell, we
179 decided to check the intracellular niche of the bacteria using LAMP-1 as a marker of SCV in
180 RAW264.7 cells (Figure 1D) and Caco-2 cells (Figure S3D) 16 h post-infection. It was
181 observed that the percent colocalization of LAMP-1 with STM *ΔompA* is less compared to
182 STM (WT) in RAW264.7 cells (Figure 1D). The colocalization with LAMP-1 increased when
183 the macrophage cells were infected with complement strain. These observations not only
184 corroborated the gradual loss of SCV membrane from its surrounding but also its enhanced
185 cytosolic localization in macrophage (Figure 1D). The PFA fixed dead bacteria lacking the
186 ability to quit vacuole was used as positive control in this study (Figure 1D). We further showed
187 the cytosolic inhabitation of *ompA* knockout bacteria in macrophage using a pH sensitive dye
188 called pH rhodo red succinimidyl ester whose fluorescence intensity increases as the pH of the
189 system decreases from neutral to acidic (Figure S4A). In comparison with wild type *Salmonella*
190 staying in the acidic pH of SCV (pH= 5 - 5.4) (Chakraborty et al., 2015), the reduction in the
191 cumulative median fluorescence intensity of STM *ΔompA* labelled with pH rhodo red
192 succinimidyl ester confirms its cytosolic abundance where the pH is almost neutral (pH= 7.2)
193 (Figure S4A) (Canton et al., 2014). The successful systemic infection caused by intracellular

194 *Salmonella* depends upon the surface accumulation as well as secretion of SPI-2 encoded
195 effector proteins from bacteria into the host cell cytoplasm with the help of a needle like
196 complex called type 3 secretion system (T3SS). The formation of this needle complex is further
197 regulated by the secretion and assembly of SPI-2 encoded translocon proteins- SseB, SseC,
198 SseD on the surface of the intravacuolar bacteria inside the lumen of SCV (Chakravortty et al.,
199 2005, Hölzer and Hensel, 2010). Since cytosolic population of STM *ΔompA* lacks the vacuolar
200 membrane, we anticipated an interruption in the accumulation of these translocon proteins on
201 bacterial surface and their secretion into the host cytosol. In line with our previous
202 observations, we found a marked reduction in the accumulation and secretion of SseC (Figure
203 S4B, S4C and S4F) and SseD (Figure S4D, S4E and S4H) on or from the surface of STM
204 *ΔompA* in comparison with wildtype bacteria into the host cytosol. In continuation of this
205 observation we found dampened expression of *sseC* (Figure S4G) and *sseD* (Figure S4I) genes
206 in intracellularly growing STM *ΔompA*. To verify whether this is a cell type specific
207 phenomenon or not, we further investigated the intracellular niche of wildtype, knockout and
208 complement strains of *Salmonella* in epithelial Caco-2 cells. The quantitative percent
209 colocalization between LAMP-1 and all three bacterial strains (Figure S3D) clearly
210 demonstrated that STM *ΔompA* comes into the cytoplasm of Caco-2 cells after being released
211 from the SCV during late phase of infection, while wild type and the complement strains
212 abstained themselves from doing so (Figure S3D). These findings were further supported by
213 chloroquine resistance assay of STM- (WT), *ΔompA*, *ΔompA*: pQE60-*ΔompA* in RAW264.7
214 (Figure 1E) and Caco-2 cells (Figure S3E). After being protonated inside SCV because of the
215 acidic pH, chloroquine can't quit the vacuole and kills the vacuolar population of *Salmonella*,
216 allowing the growth of cytosolic population. During late phase of infection (16 h post infection)
217 in RAW264.7 cells (Figure 1E) and Caco-2 cells (Figure S3E), the cytosolic abundance of STM
218 *ΔompA* was found more comparable to the wild type and complement strain. Taken together,

219 these results authenticate that, irrespective of the cell type, the intravacuolar life of the
220 intracellular *Salmonella* strongly depends upon OmpA.

221 **OmpA dependent protection of *Salmonella* against nitrosative stress inside RAW264.7**
222 **cells.**

223 The intracellular population of *Salmonella* is heavily encountered by NADPH phagocytic
224 oxidase-dependent oxidative burst and iNOS dependent nitrosative burst during early and late
225 stages of infection in macrophages respectively (Foster et al., 2003, Umezawa et al., 1997).
226 The SCV membrane protects the vacuolar niche of wild type *Salmonella* from the potential
227 threats present in the cytoplasm of macrophage in form of Reactive Oxygen Species (ROS),
228 Reactive Nitrogen Intermediates (RNI), antimicrobial peptides (AMPs), etc (Heijden et al.,
229 2015, Salcedo et al., 2002). Our study confirmed the proneness of STM *ΔompA* release from
230 SCV into the cytoplasm of macrophage and epithelial cells during the late stage of infection.
231 Hence, we assumed the increasing possibility of the mutant bacteria being targeted with ROS
232 and RNI in the cytoplasm of the macrophage, which could be a probable reason for attenuation
233 of intracellular proliferation. Our hypothesis was verified by measuring both nitrosative (Figure
234 2A – 2C) and oxidative (Figure S5A – S5C) stress response of macrophages infected with wild
235 type, knockout, and the complement strains. We quantified the extracellular (Figure 2A) [NO]
236 response produced by infected macrophages by Griess assay. It was found that during the late
237 stage of infection (16 h post-infection) the accumulation of nitrite in the culture supernatant of
238 RAW264.7 cells infected with STM *ΔompA* was significantly higher compared to the wildtype.
239 This heightened [NO] response was further revoked when the RAW264.7 cells were infected
240 with complement strain (Figure 2A). This result was further validated by quantification of
241 intracellular [NO] response using DAF2-DA (Figure 2B). Only (4.468 ± 0.774) % of wild type
242 bacteria infected macrophages produced [NO] (Figure 2B), which increased to (7.939 ± 1.056)
243 % when the cells were infected with STM *ΔompA* (Figure 2B). The percent population of cells

244 producing [NO], after being infected with complement strains (4.689 ± 0.5035) % was
245 comparable to the wild type STM infected cells (Figure 2B). During late stage of infection (16
246 h post infection) in macrophage the intracellular ROS and extracellular H_2O_2 levels were
247 estimated using H_2DCFDA (Figure S5A and S5B) and phenol red assays (Figure S5C),
248 respectively. We did not find any considerable change in the population of cells producing
249 ROS, infected with wild type (2.157 ± 0.1611)%, knockout (2.192 ± 0.2955) % and the
250 complement strains (2.61 ± 0.2244)% of *Salmonella* (Figure S5A and S5B). To validate this
251 observation, we further went ahead to check the accumulation of H_2O_2 in the culture
252 supernatants of infected RAW264.7 cells. But there was hardly any difference in H_2O_2
253 production (Figure S5C). The [NO] produced from cellular pool of L- arginine by the catalytic
254 activity of inducible nitric oxide synthase (iNOS) is further oxidized into [NO]-adducts
255 (NONOates, peroxynitrite, nitrite etc.) with the help of the superoxide ions which have higher
256 oxidation potential and bactericidal activity (Chakravortty et al., 2002). The damage that is
257 caused to bacteria by peroxynitrite ($ONOO^-$) can be monitored by the recruitment of
258 nitrotyrosine on the surface of intracellular bacteria using specific anti-nitrotyrosine antibody
259 by confocal microscopy (Figure 2C). During the late stage of infection in RAW264.7 cells, the
260 STM *ΔompA* strain showed higher surface recruitment of nitrotyrosine residues and greater
261 colocalization in comparison with the wild type bacteria (Figure 2C), indicating massive
262 damage caused by the bactericidal function of peroxynitrite. *Listeria monocytogenes* produce
263 listeriolysin O (LLO), a pore-forming toxin to degrade the vacuolar membrane to escape
264 lysosomal fusion (Ruan et al., 2016). Despite having intact OmpA on its surface, wild type
265 *Salmonella* residing in the cytoplasm due to the ectopic expression of listeriolysin O (LLO)
266 showed poor colocalization with nitrotyrosine (Figure 2C). This suggests the ability of OmpA
267 to impart defense machinery to the cytosolic population of wild type *Salmonella* against the
268 RNI. The greater recruitment of nitrotyrosine on STM *ΔompA*: *LLO* which is comparable to

269 STM *ΔompA* suggests that LLO does not play any role in modulating the activity of iNOS.
270 Consistent with this, the intracellular survival of STM (WT): *LLO* in macrophage was better
271 than STM *ΔompA* and comparable to that of wild type bacteria (Figure 2D). Taken together,
272 we show that OmpA protects intracellular wild type *Salmonella* Typhimurium against the
273 nitrosative stress of macrophages. While proliferating in macrophage it utilizes SPI-2 encoded
274 virulent factor SpiC to downregulate the activity of inducible nitric oxide synthase in SOCS-3
275 dependent manner (Uchiya and Nikai, 2008, Uchiya and Nikai, 2005). To verify whether the
276 OmpA dependent downregulation of the activity of iNOS happens in SpiC dependent manner
277 the transcript level of *spiC* was measured from wild-type and the mutant bacteria growing in
278 macrophages (Figure 2E). Unlike the wild type *Salmonella*, STM *ΔompA* was unable to
279 produce *spiC* within macrophage. The reduced expression of *spiC* by STM (WT): *LLO* and
280 bafilomycin A treated cells infected with wild-type bacteria not only shows the requirement of
281 the acidic pH of SCV for the expression of *spiC* but also indirectly authenticates the cytosolic
282 localization of STM *ΔompA*. To validate this observation the promoter activity of *spiC* was
283 measured in STM (WT) and *ΔompA* growing in stationary phase in LB media and macrophage
284 (Figure 2F) by beta-galactosidase assay. No significant change in the activity of the promoter
285 of *spiC* was observed in the wild type and mutant bacteria when grown in LB broth (Figure
286 2F) where there was no significant change in the pH. Inside the macrophage where there exists
287 a notable difference between the localization of wild type and *ompA* deficient bacteria, a
288 significant drop in the activity of the *spiC* promoter was observed in STM *ΔompA* (Figure 2F).
289 The localization of STM *ΔompA* in the cytosol of macrophage where the pH is relatively higher
290 than SCV can be held accountable for the abrogated expression of *spiC*. We observed a higher
291 488 nm/ 405 nm values of STM *ΔompA* labelled with 20 μM concentration of BCECF-AM
292 resuspended in phosphate buffer of acidic pH (range 5.5, 6, and 6.5) in comparison with STM
293 (WT) and the complemented strain (*ΔompA*: pQE60-*ompA*) (Figure 2G). Surprisingly when all

these strains were incubated separately in phosphate buffer (pH= 7) we found comparable 488 nm/ 405 nm values, which suggests the indispensable role of OmpA in the acidification of the cytosol of *S.* Typhimurium in response to extracellular acidic stress (Figure 2G).

Inhibition of the activity of iNOS improves the survival of STM *ΔompA* in *in vitro* and *in vivo* infection model.

To investigate further the pro-bacterial role of *Salmonella* OmpA against the nitrosative stress of macrophage, we treated the cells with 1400W dihydrochloride (10 µM), an irreversible inhibitor of inducible nitric oxide synthase (iNOS), the key enzyme in the production of [NO] (Figure 3A, 3C, and 3D), or mouse IFN-ɣ that upregulates the expression of iNOS (at 100 U/ mL concentration) (Figure 3B, 3C, and 3E). Inhibition of iNOS using 1400W completely restored the intracellular proliferation of STM *ΔompA* (43.61 ± 6.837) compared to the untreated reference (19.32 ± 3.913) (Figure 3A). Consistent with this finding STM *ΔompA* showed poor colocalization with nitrotyrosine under 1400W treatment (Figure 3C and 3D), which can be attributed to the poor biogenesis of RNI due to the inhibition of iNOS. Augmenting the iNOS activity of macrophage using mouse IFN-ɣ hindered the intracellular proliferation of STM *ΔompA* (12.52 ± 1.334) compared to the IFN-ɣ untreated cells (19.64 ± 2.11) (Figure 3B). The enhanced biogenesis and colocalization of nitrotyrosine with STM *ΔompA* under IFN-ɣ treatment as demonstrated by the confocal image can be taken into consideration for its higher attenuation in intracellular proliferation (Figure 3C and 3E). The reduced CFU burden of *ompA* deficient *Salmonella* in the liver, spleen, and MLN of C57BL/6 mice (compared to the wild type bacteria) strongly supports the role of OmpA in bacterial pathogenesis (Figure 3G). In our *ex vivo* studies, we established the role of OmpA in protecting the wild type *Salmonella* against the nitrosative stress of macrophages. Further, we used *iNOS*$^{-/-}$ C57BL/6 mice and wild type C57BL/6 mice treated with a pharmacological inhibitor of iNOS called aminoguanidine hydrochloride at a dose of 10 mg/ kg of body weight from 0th day (on

the day of infecting the mice) to 5th day (the day of sacrificing and dissecting the mice) (Figure 3G) (Pearse et al., 2003). We found a comparable CFU burden of wild type and *ompA* deficient bacteria in the liver, spleen, and MLN of *iNOS*$^{-/-}$ and wild type C57BL/6 mice administered with the inhibitor. The higher bacterial burden of STM *ΔompA* from the *iNOS*$^{-/-}$ and aminoguanidine-treated mice in comparison with PBS treated mice (Figure 3G) concomitantly authenticates our results obtained from *ex vivo* experiments. Likewise, use of the *gp91phox*$^{-/-}$ mice which is unable to produce ROS upon bacterial infection showed comparable CFU burden for both the wild type and *ΔompA* STM in liver, spleen, and MLN. A significantly higher bacterial burden of *ompA* deficient STM in liver of *gp91phox*$^{-/-}$ vs wild type C57BL/6 mice indicates the inability of *gp91phox*$^{-/-}$ mice to generate peroxynitrite due to dampened production of superoxide ions (ROS) (Figure3G). However, a comparable burden of STM *ΔompA* and the wild type strain in the spleen and MLN of *gp91phox*$^{-/-}$ mice and the wild type C57BL/6 mice suggests that ROS alone cannot clear the *in vivo* infection by STM *ΔompA*. Earlier we found that the infection of RAW264.7 cells with STM *ΔompA* does not induce the level of intracellular ROS. To show the role of *ompA* in *in vivo* infection of *Salmonella* Typhimurium, we challenged 4- 6 weeks old adult BALB/c and C57BL/6 mice (Figure 3H) with a lethal dose (10^8 CFU of bacteria/ animal) of wild type and knockout strains by oral gavaging. Almost 80% of BALB/c mice infected with STM *ΔompA* survived compared to the group of mice infected with wild-type bacteria (Figure 3H). On the other side, the C57BL/6 mice infected with STM *ΔompA* showed better survival and retarded death compared to the mice infected with the wild type strain, suggesting a critical role of *ompA* in infection by *Salmonella*.

OmpA dependent regulation of outer membrane permeability in *Salmonella* controls cytoplasmic redox homeostasis in response to *in vitro* nitrosative stress.

343 In a mildly acidic environment (pH= 5 – 5.5) $NaNO_2$ dissociates to form nitrous acid (HNO_2),
344 which undergoes dismutation reaction upon oxidation and eventually generates a wide range
345 of reactive nitrogen intermediates (RNI) such as, nitrogen dioxide (NO_2), dinitrogen trioxide
346 (N_2O_3), nitric oxide (NO), etc (Heaselgrave et al., 2010). After entering the bacterial cells RNIs
347 cause irreparable deleterious effects targeting multiple subcellular components such as nucleic
348 acids (cause deamination of nucleotides), proteins (disruption of Fe-S clusters, heme group;
349 oxidation of thiols and tyrosine residues), lipids (cause peroxidation), etc, and finally kill the
350 pathogen (Fang). To investigate the role of *Salmonella* OmpA against *in vitro* nitrosative stress,
351 we decided to check *in vitro* sensitivity of the wild type and *ompA* knockout strains in the
352 presence of a varying concentration (0-5 mM) of H_2O_2 (Figure S5D), $NaNO_2$ (Figure S5E), and
353 a combination of H_2O_2 and $NaNO_2$ for 12 h (Figure S5F) by CFU and resazurin test. In
354 comparison with wild-type bacteria, STM *ΔompA* did not show any significant difference in
355 viability when exposed to peroxide (Figure S5D). The knockout strain displayed a strong
356 reduction in viability compared to the wild-type bacteria at 800 μM concentration when they
357 were incubated with $NaNO_2$ alone (Figure S5E). The sensitivity of the knockout strain towards
358 acidified nitrite further increased when H_2O_2 was added to $NaNO_2$ (where the growth inhibition
359 started at 600 μM concentration) (Figure S5F). To ensure OmpA dependent protection of wild
360 type *Salmonella* against the damage caused by *in vitro* nitrosative stress, we performed a death
361 kinetics experiment with wild type and knockout bacteria in the presence of 800 μM acidified
362 nitrite (Figure 4A). Consistent with our previous observations, the knockout strain showed a
363 notable hindered growth compared to the wild type at 12 h post-inoculation. Taking the
364 impeded growth of the mutant strain in presence of *in vitro* nitrosative stress into consideration,
365 we hypothesized enhanced entry of nitrite into the *ΔompA* strain compared to the wild type. To
366 verify this, we proceeded to perform nitrite uptake assay with the wild type, knockout,
367 complement, and empty vector strain in MOPS-NaOH buffer with 200 μM initial concentration

368 of nitrite. We noticed a greater time-dependent uptake of nitrite by the *ΔompA* and empty vector
369 strain in comparison with wild type and the complemented strains (Figure 4B). To verify OmpA
370 dependent redox homeostasis of *Salmonella* in response to *in vitro* nitrosative stress, we
371 exposed both the wild type and knockout strains harboring pQE60-Grx1-roGFP2 plasmid to
372 800 μM, 1 mM, and 5 mM (Figure 4C) concentration of acidified nitrite for 15, 30, 45 and 60
373 minutes. The redox-sensitive GFP2 (roGFP2) can absorb at two wavelengths 405 nm and 488
374 nm depending upon its oxidized and reduced state respectively. It has a fixed emission at 510
375 nm (Hans Reuter et al., 2019). The glutaredoxin protein (Grx1) fused to the redox-sensitive
376 GFP2 can reversibly transfer electrons between the cellular (GSH/GSSG) pool and the thiol
377 groups of roGFP2 at a much faster rate. The ratio of fluorescence intensity of Grx-roGFP2
378 measured at 405 nm and 488 nm demonstrates the redox status of the cytoplasm of bacteria
379 (Tung Ngoc et al., 2018). In all three concentrations of acidified nitrite {800 μM, 1 mM, 5 mM
380 (Figure 4C)}, we found a time-dependent increase in the 405/ 488 ratio of Grx1-roGFP2 in
381 STM *ΔompA* strain in comparison with STM (WT) suggesting a heightened redox burst in the
382 cytoplasm of *ompA* knockout strain in response to RNI *in vitro*. Taken together, our data clearly
383 indicates the importance of OmpA in maintaining the cytosolic redox homeostasis of wild type
384 *Salmonella*. Earlier, we have noticed a significant downregulation in the transcript levels of
385 outer membrane bound larger porins (*ompC*, *ompD*, and *ompF*) compared to *ompA* in wildtype
386 *Salmonella* growing in acidic F media and RAW264.7 cells. Our previous study depicted
387 enhanced uptake of nitrite by STM *ΔompA* strain in comparison to STM (WT), which further
388 indicates increased permeability of the bacterial outer membrane. Hence, we decided to check
389 the expression of larger porins in STM *ΔompA* strain growing in *in vitro* and *ex vivo* conditions.
390 Surprisingly, in contrast to the wildtype bacteria, we have found elevated expression of *ompC*,
391 *ompD*, and *ompF* in STM *ΔompA* strain growing in nutritionally enriched LB media, nutrient-
392 depleted acidic F media (pH= 5.4), and RAW264.7 macrophage cells (Figure 4D). This

heightened expression of larger porins was revoked in the complemented strain. In this regards the enhanced outer membrane polarity of STM (WT) and *ΔompA* growing in acidic F media was further tested (during stationary phase) using a membrane-permeant negatively charged dye called $DiBAC_4$ (Figure 4E) (Marathe et al., 2010). Because of the enhanced outer membrane permeability when the negative charge of the bacterial cytosol (called polarised state) gets diminished by the inflow of cations (called depolarization), the cell allows the entry of $DiBAC_4$ which starts fluorescing after being bound to the cell membrane proteins and lipids. In contrary to the wild type and the complemented strain, the higher $DiBAC_4$ positive population and greater median fluorescence intensity of $DiBAC_4$ corresponding to STM *ΔompA* and the empty vector strain (Figure 4E) proves our hypothesis to be true. To strengthen this observation, we used another porin specific DNA binding fluorescent dye called bisbenzimide (Coldham et al., 2010) (Figure 4F). In comparison with the wild-type bacteria greater fluorescence intensity of bisbenzimide corresponding to STM *ΔompA* grown intracellularly in murine macrophages for 12 h (Figure 4G) firmly endorsed the result obtained from the *in vitro* experiment. Hence, we can conclude that in absence of *ompA* the enhanced outer membrane porosity of the bacteria depends upon elevated expression of larger porins such as *ompC*, *ompD*, and *ompF*.

The maintenance of the integrity of the SCV membrane inside RAW264.7 macrophage solely depends upon OmpA, not on other larger porins such as OmpC, OmpD, and OmpF.

To specify the sole contribution of larger porins in the increment of outer membrane porosity of STM *ΔompA*, we decided to knockout *ompC*, *ompD*, and *ompF* individually in kanamycin-resistant *ΔompA* background of *Salmonella*. We generated STM *ΔompA ΔompC* (Figure S6A), STM *ΔompA ΔompD* (Figure S6B), and STM *ΔompA ΔompF* (Figure S6C). We further investigated the intracellular niche of these double knockout bacterial strains in RAW264.7

418 cells during the late phase of infection (16 h post-infection). In line with our previous finding,
419 compared to the wild type bacteria, STM *ΔompA* showed poor colocalization with SCV marker
420 LAMP-1 (Figure 5A and 5B). Surprisingly, the drastic loss of SCV membrane from the
421 surroundings of STM *ΔompA ΔompC*, *ΔompA ΔompD*, and *ΔompA ΔompF* as demonstrated by
422 their poor colocalization with LAMP-1 (Figure 5B), indicating the cytosolic localization of
423 these double knockout strains in macrophage during the late phase of infection. The reduced
424 colocalization of STM (WT) expressing LLO (which usually stays in the cytoplasm) with
425 LAMP-1 (Figure 5A and 5B) authenticates the cytosolic phenotype of the double knockout
426 strains. To rule out the possibility that the lack of OmpC, OmpD, and OmpF also contributes
427 to the respective phenotypes of STM *ΔompA ΔompC*, *ΔompA ΔompD*, and *ΔompA ΔompF*
428 (Figure 5A and 5B), we generated single knockout strains of *Salmonella* lacking *ompC* (Figure
429 S6D), *ompD* (Figure S6E), and *ompF* (Figure S6F) and observed that the STM *ΔompC*,
430 *ΔompD*, and *ΔompF* strains colocalized with LAMP-1 similarly with that of the wild type strain
431 (Figure 5C and 5D). Hence, it can be concluded that the maintenance of the vacuolar life of
432 wild type *Salmonella* depends on OmpA and not on OmpC, OmpD, and OmpF. A decreased
433 recruitment of nitrotyrosine on STM *ΔompC*, *ΔompD*, and *ΔompF* in comparison with STM
434 *ΔompA* while growing intracellularly in RAW264.7 cells further supports the presence of
435 undamaged SCV membrane around them (Figure S7A). The *in vitro* sensitivity of STM
436 *ΔompC*, *ΔompD*, and *ΔompF* against the acidified nitrite was also checked (Figure S7B). It
437 was observed that, unlike the *ompA* deficient strain of *Salmonella*, the ability of STM *ΔompC*,
438 *ΔompD*, and *ΔompF* to withstand the bactericidal effect of acidified nitrite is comparable with
439 the wild type bacteria (Figure S7B). To further support this observation, we checked the
440 consumption of nitrite by STM *ΔompC*, *ΔompD*, and *ΔompF* (Figure S7C). It was found that
441 in comparison to STM *ΔompA* strain, *ΔompC*, *ΔompD*, and *ΔompF* are more efficient in

442 restricting the entry nitrite (Figure S7C) which can be attributed to their better survival in the
443 presence of acidified nitrite.

444 **In the absence of OmpA, porins OmpC and OmpF enhance the susceptibility of**
445 ***Salmonella* against nitrosative stress of RAW264.7 cells.**

446 To dissect the role of each larger porin namely OmpC, OmpD, and OmpF in the entry of nitrite
447 into bacteria during the absence of OmpA, we performed nitrite uptake assay using the double
448 knockout bacterial strains STM *ΔompA ΔompC*, *ΔompA ΔompD*, and *ΔompA ΔompF* (Figure
449 6A). In comparison with the wild type bacteria, the rapid disappearance of nitrite which
450 corroborates substantial nitrite uptake from the media by STM *ΔompA* and *ΔompA ΔompD*
451 demonstrates the involvement of OmpC and OmpF (acquired by both STM *ΔompA* and *ΔompA*
452 *ΔompD* strains) in this entry process (Figure 6A). This result was further validated by the
453 measurement of the reduced *in vitro* percent viability of STM *ΔompA* and *ΔompA ΔompD* in
454 comparison with wildtype, *ΔompA ΔompC* and *ΔompA ΔompF* in presence of acidified nitrite
455 (800 μM) (Figure 6B). Using the *ex vivo* system of infection in murine macrophage, we have
456 found enhanced recruitment of nitrotyrosine on STM *ΔompA* and *ΔompA ΔompD* as depicted
457 by their higher colocalization in comparison with wildtype, *ΔompA ΔompC*, and *ΔompA*
458 *ΔompF* (Figure 6C). The intracellular nitrosative burst of macrophage infected with STM
459 (WT), *ΔompA, ΔompA ΔompC, ΔompA ΔompD*, and *ΔompA ΔompF* was tested using DAF2DA
460 (Figure 6E). Only 7.35% of macrophage infected with wild-type bacteria produced [NO],
461 which is comparable to STM *ΔompA ΔompC* (6.12%) and *ΔompA ΔompF* (3.4%) infected
462 macrophage population producing [NO]. The enhanced median fluorescence intensity of
463 DAF2DA and greater percent population of infected macrophage corresponding to STM
464 *ΔompA* (12.79%) and *ΔompA ΔompD* (13.99%) (Figure 6E) strengthens the conclusion
465 obtained from confocal data (Figure 6C). This data was further verified by the attenuated
466 intracellular proliferation of STM *ΔompA* and *ΔompA ΔompD* inside RAW264.7 cells unlike

467 STM (WT), *ΔompA ΔompC*, and *ΔompA ΔompF* whose improved intracellular survival can be
468 attributed to reduced recruitment of nitrotyrosine (Figure 6C and 6D). Taken together, it can be
469 concluded that in absence of OmpA, the elevated expression of larger porins OmpC and OmpF
470 on the bacterial outer membrane helps in the entry of nitrite from outside within the bacterial
471 cytoplasm and makes the bacteria highly susceptible to the intracellular nitrosative burst.

472 **Discussion**

473 *Salmonella* Typhimurium, a gram-negative enteric bacterial pathogen belonging to the family
474 *Enterobacteriaceae*, experiences a wide range of environmental stresses during its extracellular
475 as well as, intracellular life cycle. While infecting a human host the bacteria are exposed to
476 varied adverse environments such as acid stress in the stomach, bile salt stress in the duodenum,
477 short-chain fatty acid, and oxygen depletion stress in the ileum, cationic antimicrobial peptides
478 in the intestinal epithelial cell linings, etc. These challenges are overcome by *Salmonella* either
479 by using EnvZ/OmpR, PhoPQ two-component systems or by global stress response regulators
480 RpoS, Fur proteins (Rychlik and Barrow, 2005).

481 While infecting macrophage or epithelial cells, *Salmonella* staying in *Salmonella* containing
482 vacuole (SCV) undergoes nutrient limitation, ion depletion (Mg^{2+}, Fe^{3+}, PO_4^{3-}), and low pH
483 stress respectively (Eriksson et al., 2003, Hautefort et al., 2008). By inducing significant
484 changes in their metabolic status such as upregulation of Enter-Duodoroff (which prefers
485 alternative carbon source such as gluconate) and aromatic amino acid biosynthesis pathways,
486 downregulation of purine/ pyrimidine biosynthesis pathway (because of the slow rate of
487 replication in SCV), blocking the expression of H+/ATPase pumps (to stop the influx of H+
488 ions) and by increasing the synthesis of specific ion transporters on its surface wildtype
489 *Salmonella* survives efficiently in SCV (Eriksson et al., 2003). During systemic infection in
490 macrophage and epithelial cells, *Salmonella* is further challenged by cationic antimicrobial

491 peptides, reactive oxygen, and nitrogen species respectively (Gogoi et al., 2019, Balakrishnan
492 et al., 2016, Chakraborty et al., 2014), which are successfully encountered by the bacteria with
493 the impermeable membranous barrier of SCV and SPI-2 encoded effectors proteins (Heijden
494 et al., 2015, Das et al., 2009). Further, the compositions, arrangements, and heterogeneity of
495 the outer membrane lipids and proteins play a crucial role in the maintenance of the
496 pathogenesis of gram-negative bacteria. Recent studies have suggested that bacterial pathogens
497 (such as *Acinetobacter baumannii*, *E. coli*, *K. pneumoniae* etc) can restrict the entry of toxic
498 molecules such as antibiotics and cationic antimicrobial peptides either by changing the outer
499 membrane permeability (Smani et al., 2014, Ghai and Ghai, 2018), or by augmenting omptins/
500 proteases that degrade the antimicrobial peptides (Kukkonen and Korhonen, 2004). The
501 alteration in the outer membrane permeability as well as integrity of gram-negative pathogen
502 is strictly regulated by the core oligosaccharide composition of outer membrane
503 lipopolysaccharide and differential expression of outer membrane porins (Ebbensgaard et al.,
504 2018, Iyer et al., 2018, Choi and Lee, 2019).

505 OmpA, OmpC, OmpD, OmpF, and PhoE, the predominantly found porins on the outer
506 membrane of *Salmonella* Typhimurium, are involved in a wide range of functions. OmpA
507 tightly holds the outer membrane of the bacteria to the peptidoglycan layer of the cell wall and
508 hence, deletion of OmpA aggravates the biogenesis of outer membrane vesicles (OMV) (Park
509 et al., 2012, Nevermann et al., 2019). OmpD, the most abundant porin on *Salmonella* outer
510 membrane, is involved in the uptake of H_2O_2 (Calderón et al., 2011). OmpC in conjunction
511 with OmpF contributes to the acquisition of cations, whereas PhoE majorly helps in the uptake
512 of negatively charged phosphate groups (Ipinza et al., 2014). The correlation between outer
513 membrane porins and *Salmonella* pathogenesis has been poorly understood due to the lack of
514 extensive studies. Earlier Heijden *et al.* showed that HpxF$^-$ *Salmonella* altered outer membrane
515 permeability by reciprocally regulating the expression of OmpA and OmpC when exposed to

516 H_2O_2 (Heijden et al., 2016). OmpA deficient *Salmonella* was found to be incapable of reaching
517 the mouse brain (Chaudhuri et al., 2018). Deletion of *ompD* from the genome of *Salmonella*
518 made it hyper-proliferative in RAW264.7 macrophages and BALB/c mouse models (Ipinza et
519 al., 2014). In this study, we delineated the individual contributions of OmpA, OmpC, OmpD,
520 and OmpF in *Salmonella* pathogenesis. Our study not only revealed the role of porins in the
521 maintenance of the intravacuolar life of wildtype *Salmonella* Typhimurium but also deciphered
522 their role in the regulation of outer membrane permeability and bacterial resistance to the
523 nitrosative stress of macrophage.

524 We have found a time-dependent steady decrease in the transcript levels of *ompC*, *ompD*, and
525 *ompF* (Figure S1B, S1C, S1D) in *Salmonella* growing in RAW264.7 cells. On the contrary, the
526 consistently elevated expression of *ompA* during the late phase of infection in RAW264.7 cells
527 (9 h and 12 h post-infection) (Figure S1A) suggested the importance of this porin in bacterial
528 survival inside the macrophage. Our observations corroborate the findings of Eriksson *et al.*,
529 and Hautefort *et al* (Eriksson et al., 2003, Hautefort et al., 2008). Unlike other major porins,
530 OmpA has a small pore size and a unique periplasmic domain (Figure S1B, S1D, 1F, and 1H)
531 which can act as a gate to restrict the entry of many toxic molecules (Heijden et al., 2016).
532 Hence it can be concluded that wild type bacteria growing in a nutrient-depleted stressed
533 environment of SCV within the macrophage, where the bacterial growth is severely challenged
534 by acidic pH, would always prefer OmpA a porin with a smaller pore size and periplasmic
535 gating mechanism on its surface to restrict the entry of excess H+ ions. OmpA, one of the most
536 abundant porins of the outer membrane of *E. coli* K1, the causative agent of neonatal
537 meningitis, is highly conserved in the family of *Enterobacteriaceae* (Krishnan and Prasadarao,
538 2012). Besides its structural role in the outer membrane, OmpA of *E. coli* K1 and *Enterobacter*
539 *sakazakii* has been reported to be involved in the invasion of hBMEC cells, and INT407 cells
540 by multiple studies (Mohan Nair and Venkitanarayanan, 2007, Mittal et al., 2011, Singamsetty

541 et al., 2008). OmpA of *E. coli* K1 not only augments complement resistance by recruiting C4
542 binding protein (C4BP) on the surface of the bacteria (Abreu and Barbosa, 2017) but also
543 abrogates their intracellular survival in murine and human macrophages (Sukumaran et al.,
544 2003). In our study, the OmpA deficient strain of *Salmonella* has shown a higher inclination
545 towards phagocytosis and severe attenuation in intracellular proliferation in macrophages.
546 Surprisingly, on the other hand, deletion of *ompA* makes *Salmonella* invasion deficient and
547 hyper-proliferation in epithelial cells. The successful systemic infection of *Salmonella* in
548 macrophages as well as in epithelial cells depends upon its intravacuolar inhabitation. The
549 acidification inside the SCV is a prerequisite for the synthesis and secretion of SPI-2 encoded
550 virulent proteins which are required for the successful proliferation of *Salmonella* (Chakraborty
551 et al., 2015). Mild tampering with the integrity of SCV may create unusual outcomes in the
552 bacterial burden of the cells. Earlier it has been reported that the intracellular proliferation of
553 *sifA* mutant of *Salmonella,* which comes into the cytoplasm after quitting SCV, was severely
554 abrogated in macrophages and aggravated in the cytosol of epithelial cells (Salcedo et al.,
555 2002). The introduction of point mutations in the Rab5 or Rab7 proteins (markers of SCV) can
556 also trigger the release of wild-type bacteria from SCV to the cytosol of epithelial cells
557 (Brumell et al., 2002). Our immunofluorescence microscopy data along with the result from
558 chloroquine resistance assay showed the cytosolic localization of *ompA* deficient strain of
559 *Salmonella* in macrophage as well as in epithelial cells. STM *ΔompA* that stay into the neutral
560 pH of cytoplasm has shown reduced colocalization with SseC and SseD, two translocon
561 proteins, whose synthesis, surface accumulation, and secretion into the host cell cytoplasm
562 depend upon the acidic pH of SCV and SPI-2 encoded T3SS needle complex (Chakravortty et
563 al., 2005), further validates our observation. Moreover, the result obtained from intracellular
564 proliferation assay of STM *ΔompA* in macrophage and epithelial cells and the
565 immunofluorescence microscopy data on vacuolar/ cytosolic niche are consistent with the

566 available literatures. Hence, to best of our knowledge, this is the first report commenting on
567 the ability of OmpA to maintain the integrity and stability of *Salmonella* containing vacuole.

568 The SCV membrane functions as a protective barrier around the wild type bacteria. Once the
569 intactness of the SCV membrane is lost, the bacteria will eventually be exposed to the threats
570 present in the cytosol in form of ROS and RNI (Heijden et al., 2015). Hence, the oxidative and
571 nitrosative burst of macrophage infected with wild type, and the *ompA* knockout strain of
572 *Salmonella* were checked. Surprisingly, we found a remarkable rise in the level of intracellular
573 as well as, extracellular [NO] of macrophages infected with STM *ΔompA*, indicating the
574 protective role of OmpA against the nitrosative stress of macrophages. In continuation with the
575 previous observation, STM *ΔompA* which has already quit the SCV and staying in cytosol
576 showed greater colocalization with nitrotyrosine when compared with the wild type bacteria
577 which is protected inside the vacuole. A decreased recruitment of nitrotyrosine on STM (WT):
578 *LLO* staying in the cytoplasm of macrophage due to ectopic expression of listeriolysin O and
579 their better survival in macrophage in comparison with STM *ΔompA* further strengthen the
580 conclusion. The alteration in the proliferation of STM *ΔompA* in macrophages and the
581 recruitment profile of nitrotyrosine upon manipulation of iNOS activity using specific
582 irreversible inhibitor 1400W dihydrochloride and activator IFN-ɣ fell in line with the previous
583 results. Wild type *Salmonella*, with the help of its pathogenicity island (SPI)- 2 encoded
584 virulent factor SpiC activates suppressor of cytokine signaling 3 (SOCS-3) which inhibit IFN-
585 γ signaling and thus eventually represses the activation of iNOS (Das et al., 2009, Uchiya and
586 Nikai, 2005). As discussed earlier, the acidification of the SCV compartment acidifies the
587 cytosol of wildtype *Salmonella*. It is essential for the synthesis and secretion of SPI-2 effector
588 proteins into the host cell's cytoplasm (Chakraborty et al., 2015). We have also found that STM
589 *ΔompA,* which stays in the neutral pH of cytoplasm in macrophages after quitting SCV, cannot
590 produce SpiC. Further, we checked the promoter activity of *spiC* in wild-type and mutant

591 bacteria growing both extracellularly and intracellularly by β galactosidase assay. Compared
592 to the intracellularly growing STM *ΔompA*, the higher activity of *spiC* promoter in wild-type
593 *Salmonella* simultaneously supports the cytosolic inhabitation of STM *ΔompA* and answers the
594 reason behind the nitrosative burst of macrophage. The downregulation of SPI-2 encoded gene
595 *spiC* in STM *ΔompA* can also be attributed to its incompetence to acidify its cytosol in response
596 to extracellular acidic response determined by a higher 488 nm/ 405 nm ratio of BCECF-AM.
597 But strikingly, STM *ΔompA* was unable to induce intracellular and extracellular ROS
598 production while infecting macrophages. NADPH phagocytic oxidase is the key enzyme of
599 macrophages involved in the synthesis of superoxide ions. It is a multimeric protein consisting
600 of two membrane-bound subunits, such as gp91^{phox}, p22^{phox}, and four cytosolic subunits, such
601 as p47^{phox}, p40^{phox}, p67^{phox,} and RacGTP (Panday et al., 2015). In continuation with our previous
602 observations, we found poor colocalization of gp91^{phox} with STM (WT) and *ΔompA* in
603 macrophages during the late phase of infection (data not shown). Wild-type *Salmonella* can
604 inhibit the recruitment of NADPH oxidase on the surface of the SCV membrane with the help
605 of SPI-2 encoded type 3 secretion system (Gallois et al., 2001). The restriction in the
606 recruitment of NADPH oxidase on the surface of the *ompA* knockout bacteria lacking SCV
607 membrane and staying in the cytosol is why the dampened oxidative stress inside the infected
608 macrophage. On the contrary, the ability of iNOS to maintain its uninterrupted catalytic activity,
609 despite being recruited on the cortical actin of macrophage (Webb et al., 2001), is the most
610 probable reason behind elevated production of RNI in RAW264.7 cells infected with STM
611 *ΔompA*. To investigate the role of OmpA in the establishment of *in vivo* infection by wildtype
612 *Salmonella* Typhimurium we have used 4 to 6 weeks old *Nramp*$^{-/-}$ C57BL/6 and BALB/c mice.
613 The better survival of the mice infected with *ompA* deficient strains of *Salmonella*, which was
614 attributed to the reduced bacterial burden in the liver, spleen, and MLN, finally endorsed the
615 essential role of OmpA in the *in vivo* infection of *Salmonella*. Administration of iNOS inhibitor

616 aminoguanidine hydrochloride by intraperitoneal injection or direct oral infection of *iNOS*$^{-/-}$
617 mice diminished the *in vivo* attenuation of STM *ΔompA,* suggesting OmpA dependent
618 protection of wildtype bacteria against nitrosative stress *in vivo*. The comparable CFU burden
619 of STM (WT) and *ΔompA* in *gp91phox*$^{-/-}$ C57BL/6 mice, which is unable to produce ROS, can
620 be accounted for the abrogated peroxynitrite response (Zielonka et al., 2016, Vlahos R,
621 Stambas J, Bozinovski S, Broughton BRS, Drummond GR, 2011). Acidified nitrite generating
622 a wide range of reactive nitrogen intermediates (RNI) such as nitrogen dioxide (NO_2),
623 dinitrogen trioxide (N_2O_3), nitric oxide (NO), etc., are extensively used for assessing *in vitro*
624 viability of bacteria and fungi (Heaselgrave et al., 2010, Weller et al., 2001). After entering the
625 bacterial cells, RNIs cause enormous irreparable damages to multiple subcellular components
626 such as nucleic acids (cause deamination of nucleotides), proteins (disruption of Fe-S clusters,
627 heme group; oxidation of thiols and tyrosine residues), lipids (cause peroxidation), etc., and
628 eventually destroy the pathogen. (Fang) The enhanced sensitivity of STM *ΔompA* against
629 acidified nitrite and combination of acidified nitrite with peroxide, which generates
630 peroxynitrite (Kono, Y., Shibata, H., Adachi, K., Tanaka) suggested increased entry of nitrite
631 in the knockout strain comparison with wildtype bacteria. The faster depletion of nitrite from
632 the media having STM *ΔompA* strongly supported our hypothesis. The time-dependent gradual
633 increase in 405/ 488 ratio of pQE60-Grx1-roGFP2 harboured by STM *ΔompA* under all the
634 tested concentrations of acidified nitrite proved the loss of redox homeostasis in STM *ΔompA*.

635 As discussed earlier, the outer membrane of Gram-negative bacteria acts as an impermeable
636 barrier to many toxic compounds (including antibiotics, bile salts, cationic antimicrobial
637 peptides, reactive oxygen species, abnormal pH, osmotic stress, etc.) and protect the bacteria
638 from many environmental threats during its extracellular and intracellular survival. In the
639 absence of OmpA, the alleviation in outer membrane integrity was speculated by the enhanced
640 entry of nitrite. The greater uptake of $DiBAC_4$ (measure the cell membrane depolarisation) and

641 bisbenzimide (binds to the DNA) by the *ompA* deficient strain of *Salmonella* confirmed our
642 speculation. To rationalize the enhanced uptake of fluorescent probes by STM *ΔompA,* we
643 checked the expression of larger porins such as *ompC*, *ompD*, and *ompF* in wild-type, mutant,
644 and complemented strains of *Salmonella* growing in LB broth, F media, and RAW264.7
645 macrophage. We found a remarkable increase in the expression of the larger porins in the
646 knockout strain (lacking OmpA) compared to wild type and complement strain. Hence, we
647 conclude that OmpA regulates the outer membrane integrity of *Salmonella*. When OmpA is
648 deleted, the increased expression of larger porins such as OmpC, OmpD, and OmpF reduces
649 the intactness and stability of the outer membrane and makes it permeable to small molecules
650 like nitrite. The reduction in the expression of OmpC, OmpD, and OmpF in the *ompA*
651 complemented strain of *Salmonella* suggests the strategic utilization of OmpA by the bacteria
652 to survive in a stressed environment. This conclusion can be extrapolated to understand the
653 reason behind enhanced recruitment of nitrotyrosine on STM *ΔompA* compared with STM
654 (WT): *LLO* in macrophage during the late phase of infection. Despite having cytosolic niche
655 STM (WT): *LLO* has intact OmpA in its outer membrane, unlike STM *ΔompA*, which maintains
656 the integrity and stability of the outer membrane and prohibits the entry of peroxynitrite.

657 To ascertain the individual contribution of the larger porins such as *ompC*, *ompD*, and *ompF* in
658 the entry of nitrite in *ompA* deficient bacteria, we constructed *ompC*, *ompD*, and *ompF* single
659 and double knockout strains in wild type and *ompA*$^{-}$ background of *Salmonella*, respectively.
660 The cytosolic localization of double knockout strains, namely STM *ΔompA ΔompC*, *ΔompA*
661 *ΔompD*, and *ΔompA ΔompF* and vacuolar imprisonment of the single knockout strains lacking
662 *ompC*, *ompD*, and *ompF* respectively provided vital support to our previous conclusion on the
663 dependence of SCV integrity and stability on OmpA. Under the *in vitro* challenge of acidified
664 nitrite, the better survival of STM *ΔompC*, *ΔompD*, and *ΔompF* in comparison with *ΔompA* not
665 only suggested the abrogated consumption of nitrite but also indisputably established the

666 paramount importance of OmpA in the maintenance of the outer membrane permeability of
667 wildtype *Salmonella.* STM *ΔompA ΔompD,* which possesses intact OmpC and OmpF on their
668 outer membrane, showed enhanced nitrite consumption and higher sensitivity towards *in vitro*
669 nitrosative stress (800 µM of acidified $NaNO_2$). In comparison with STM *ΔompA ΔompC* and
670 *ΔompA ΔompF,* which also stay in the cytosol of murine macrophages, greater recruitment of
671 nitrotyrosine on STM *ΔompA ΔompD* is considered as the sole reason behind their low
672 proliferation in murine macrophage. These results were further supported by the inability of
673 STM *ΔompA ΔompC* and *ΔompA ΔompF* to induce heightened [NO] response while staying
674 inside the macrophage, unlike STM *ΔompA ΔompD*. These results collectively endorse the
675 pivotal role of OmpC and OmpF in the entry of nitrite in *ompA* deficient *Salmonella*
676 Typhimurium by increasing the permeability and worsening the integrity of the bacterial outer
677 membrane.

678 To summarize, our study claims that the OmpA of Salmonella Typhimurium is a versatile
679 protein with many activities. The deletion of *ompA* from *Salmonella* disrupts the stability of
680 SCV and imposes significant paradoxical consequences on the intracellular proliferation of
681 bacteria. We further proposed an intelligent strategy of the wild-type *Salmonella* Typhimurium
682 to utilize OmpA to maintain the outer membrane's integrity and permeability to fight against
683 macrophages' nitrosative stress.

684

685 **Abbreviations**

686 STM: *Salmonella* Typhimurium

687 OmpA: Outer membrane protein A

688 OmpC: Outer membrane protein C

OmpD: Outer membrane protein D

OmpF: Outer membrane protein F

LLO: Listeriolysin O

SCV: *Salmonella* containing vacuole

LAMP-1: Lysosome associated membrane protein-1

iNOS: Inducible nitric oxide synthase

RNI: Reactive nitrogen intermediates

ROS: Reactive oxygen species

RFP: Red fluorescent protein

roGFP2: Redox sensitive green fluorescent protein

Materials and Methods

Bacterial strains, media, and culture conditions

The wild type (WT) bacteria *Salmonella enterica* serovar Typhimurium [STM- (WT)] strain 14028S used in this study was a generous gift from Professor Michael Hensel, Max Von Pettenkofer-Institute for Hygiene und Medizinische Mikrobiologie, Germany. The bacterial strains were revived from glycerol stock (stored in -80^{0}C) and plated either only on LB agar (purchased from HiMedia) or LB agar along with appropriate antibiotics like- kanamycin (50 µg/mL), ampicillin (50 µg/mL), Chloramphenicol (25 µg/mL), kanamycin and ampicillin (both 50 µg/mL), Kanamycin and Chloramphenicol (Kanamycin= 50 µg/mL, Chloramphenicol= 25 µg/mL) for wild type, knockout (single and double), complement and mCherry expressing strains respectively. *Salmonella- Shigella* agar was used for plating of cell lysates/ cell suspensions to calculate the bacterial burden in infected cell lines and several organs of infected

mice respectively. Bacterial LB broth cultures were grown in a shaker incubator at 180 rpm either 37^0C for normal wild type and knockout strains or 30^0C for the strains having temperature-sensitive pKD46 plasmid or the strains harboring pQE60-Grx1-roGFP2 plasmid and undergoing IPTG (concentration= 500 µM) treatment. For growth curve experiments and *in vitro* RNA extraction studies, a single colony was inoculated in 5mL of LB broth and grown overnight with or without antibiotics at 37^0C. Overnight-grown stationary phase bacteria were sub-cultured at a ratio of 1: 100 in freshly prepared LB or minimal N salt media and kept in a 37^0C shaker incubator. At different time intervals aliquots were taken for RNA isolation, serial dilution, plating, and measurement of $[OD]_{600nm}$ by TECAN 96 well microplate reader. The complete list of strains and plasmids have been listed below. (Description in Table-1) Dead bacteria used in several sets of experiments were produced from viable wild-type bacteria either heating at 65^0C for 20 minutes or by treating the bacteria with 3.5% paraformaldehyde for 30 minutes.

Eukaryotic cell lines and growth conditions

The murine macrophage-like cell line RAW 264.7, human cervical adenocarcinoma cell line HeLa, human colorectal adenocarcinoma cell line Caco-2, were maintained in Dulbecco's Modified Eagle's Media (Sigma-Aldrich) supplemented with 10% FCS (Fetal calf serum, Gibco) at 37^0C temperature in presence of 5% CO_2. Human monocyte cell line U937 cells were maintained in Roswell Park Memorial Institute 1640 media (Sigma-Aldrich) supplemented with 10% FCS (Fetal calf serum, Gibco). For polarizing the Caco-2 cells, DMEM media was further supplemented with 1% non-essential amino acid solution (Sigma-Aldrich). Phorbol Myristate Acetate (Sigma-Aldrich) (concentration- 20 ng/ mL) was used for the activation of U937 cells for 24 hours at 37^0C temperature in presence of 5% CO_2, followed by the replacement of the media carrying PMA with normal RPMI supplemented with 10% FCS and further incubating the cells for 24 hours before starting the experiments.

Construction of *ompA, ompC, ompD,* & *ompF* knockout strains of *Salmonella*

The knockout strains of Salmonella *enterica* serovar Typhimurium (strain 14028S) were made using one step chromosomal gene inactivation method demonstrated by Datsenko and Wanner (Datsenko and Wanner, 2000). Briefly, STM (WT) was transformed with pKD46 plasmid, which has a 'lambda red recombinase system' under arabinose inducible promoter. The transformed cells were grown in LB broth in the presence of ampicillin (50 µg/mL) and 50 mM arabinose at 30^0C until the $[OD]_{600nm}$ reached 0.35 to 0.4. Electrocompetent STM pKD46 cells were prepared after washing the bacterial cell pellet thrice with double autoclaved chilled Milli Q water and 10% (v/v) glycerol. Finally, the electrocompetent STM pKD46 cells were resuspended in 50 µL of 10% glycerol. Kanamycin resistant gene cassette (Kan^R, 1.6kb- for knocking out *ompA, ompD*) and chloramphenicol resistant gene cassette (Chl^R, 1.1 kb- for knocking out *ompC, ompD* & *ompF*) were amplified from pKD4 and pKD3 plasmids, respectively using knockout primers (Table-2). The amplified Kan^R and Chl^R gene cassettes were subjected to phenol-chloroform extraction and electroporated into STM (WT) pKD46. The transformed cells were plated on LB agar with kanamycin (50 µg/mL) for selection of *ΔompA, ΔompD* strains and LB agar with chloramphenicol (25 µg/mL) for selection of *ΔompC, ΔompD,* and *ΔompF* strains. The plates were further incubated overnight at 37^0C. The knockout colonies were confirmed by confirmatory and kanamycin/ chloramphenicol internal primers (Table-2).

Construction of *ompA* complemented strain of *Salmonella*

For making the complemented strain, the first *ompA* gene was amplified with *ompA* cloning primers (Description in Table-2) by colony PCR. The amplified PCR product, purified by phenol-chloroform extraction, was subjected to restriction digestion by NcoI (NEB) and HindIII (NEB) in CutSmart buffer (NEB) at 37^0C for 2-3 h along with the empty pQE60 vector

backbone. Double digested insert and vector were subjected to ligation by a T_4 DNA ligase in 10X ligation buffer (NEB) overnight at 16^0C. The ligated product, as well as the empty vector, were transformed into STM *ΔompA* strain separately to generate complemented and empty vector strains. Complementation was initially confirmed by colony PCR with cloning and *ompA* internal primers (data not shown) and finally by restriction digestion of recombinant plasmid. The expression level of *ompA* in the knockout, complemented, and empty vector strains were further confirmed by RT PCR using *ompA* specific RT primers (Description in Table-2).

Construction of *ΔompA ΔompC, ΔompA ΔompD,* & *ΔompA ΔompF* double knockout strains of *Salmonella*

The double knockout strains of Salmonella *enterica* serovar Typhimurium (strain 14028S) were made by slightly modifying one step chromosomal gene inactivation strategy demonstrated by Datsenko and Wanner (Datsenko and Wanner, 2000). Briefly, STM *ΔompA*, where the *ompA* gene has already been replaced with a kanamycin-resistant gene cassette, was transformed with pKD46 plasmid. The transformed cells were grown in LB broth in presence of ampicillin (50 μg/mL) and 50 mM arabinose at 30^0C until $[OD]_{600nm}$ reached 0.35 to 0.4. Electrocompetent STM *ΔompA* pKD46 cells were made using the protocol mentioned above. Chloramphenicol resistant gene cassette (Chl^R, 1.1 kb) was amplified from pKD3 plasmid using knockout primers having a stretch of oligos at the 5' end homologous to the flanking region of the target genes- *ompC*, *ompD*, *ompF* (Table-2). The amplified Chl^R gene cassette was subjected to phenol-chloroform extraction and electroporated into STM *ΔompA* pKD46. The transformed cells were plated on LB agar with kanamycin (50 μg/mL) and chloramphenicol (25 μg/mL) both for selection of double knockout strains (*ΔompA ΔompC*, *ΔompA ΔompD*, and *ΔompA ΔompF*). The plates were further incubated overnight at 37^0C. The knockout colonies were confirmed by confirmatory primers (Table-2).

RNA isolation and RT PCR

The bacterial cell pellets were lysed with TRIzol reagent (RNAiso Plus, Takara) and stored at -80^{0}C overnight. The lysed supernatants were further subjected to chloroform extraction followed by precipitation of total RNA by adding an equal volume of isopropanol. The pellet was washed with 70% RNA grade ethanol, air-dried and suspended in 20 µL of DEPC treated water. The concentration of RNA was measured in nano-drop and analyzed on 1.5% agarose gel to assess the quality of RNA. To make cDNA, 3 µg of RNA sample was subjected to DNase treatment in presence of DNase buffer (Thermo Fischer Scientific) at 37^{0}C for 2 h. The reaction was stopped by the addition of 5mM Na_2EDTA (Thermo Fischer Scientific), followed by heating at 65^{0}C for 10 min. The samples were incubated with random hexamer at 65^{0}C for 10 min, and then supplemented with 5X RT buffer, RT enzyme, dNTPs, and DEPC treated water at 42^{0}C for 1 h. Quantitative real-time PCR was done using SYBR/ TB Green RT PCR kit (Takara Bio) in Bio-Rad real-time PCR detection system and the expression level of target genes was measured using specific RT primers (Table-2). 16S rRNA was used to normalize for the expression levels of the target genes.

Percent phagocytosis calculation/ invasion assay

1.5 to 2 X 10^5 cells (RAW264.7, U937, Caco-2, and HeLa) were seeded into the wells of 24 well plates and incubated for 6-8 h at 37^{0}C in presence of 5% CO_2. The protocol for calculating percent phagocytosis by macrophage cells has been modified a little, as demonstrated earlier (Balakrishnan et al., 2016). Briefly, the phagocytic macrophage cells (RAW264.7 and activated U937 cells) were infected with 10- 12 h grown stationary phase cultures of STM (WT), *ΔompA*, *ΔompA*: pQE60-*ompA* and *ΔompA*: pQE60 at MOI 10. For assays with the complemented strains, the strains were incubated with 10% mouse complement sera for 2 h before the experiment, and MOI 50 was used for the infection. Non-phagocytic epithelial cells (Caco-2

and HeLa cells) were infected with the cells from 3 to 4 h old log phase culture of all four bacterial strains at the same MOI. The attachment of bacteria to the cell surface was increased by centrifuging the cells at 800 rpm for 5 min, followed by incubating the infected cells at 37^0C in presence of 5% CO_2 for 25 min. Next, the cells were washed thrice with PBS to remove unattached bacteria and subjected to 100 μg/ mL and 25 μg/ mL concentration of gentamycin treatment for 1 h each. 2 h post-infection, the cells were lysed with 0.1% triton-X-100. The lysate was plated on *Salmonella- Shigella* agar and the corresponding CFUs were enumerated. Percent phagocytosis (for phagocytic macrophage cells)/ percent invasion (for non-phagocytic epithelial cells) was determined using the following formula-

Percent phagocytosis/ percent invasion= [CFU at 2 h]/ [CFU of pre-inoculum] X 100

Adhesion assay

The protocol of adhesion assay was as described before (Garai et al., 2016). Briefly, 1.5 to 2 X 10^5 cells (RAW264.7 and HeLa) were seeded on the top of sterile glass coverslips. Phagocytic macrophage cells (RAW264.7) were infected with 10- 12 h old stationary phase culture of STM (WT), *ΔompA*, *ΔompA*: pQE60-*ompA* and *ΔompA*:pQE60 at MOI 50. Non-phagocytic epithelial cells (HeLa) were infected with 3 -4 hours old log phase culture of all four bacterial strains at the same MOI. After centrifuging the cells at 800 rpm for 5 min, the infected cells were incubated at 37^0C temperature in presence of 5% CO_2 for 15 minutes (for RAW264.7 cells) and 25 minutes (for HeLa cells), respectively. After the incubation period, the cells were washed twice with sterile PBS and fixed with 3.5% PFA. To visualize the externally attached bacteria, the cells were primarily treated with anti-*Salmonella* antibody raised in rabbit (dilution 1: 100, duration 6 to 8 hours at 4^0C temperature), which was followed by the treatment of the cells with secondary antibody conjugated to an appropriate fluorophore (dilution 1: 200, duration 1 hour at room temperature), dissolved in 2.5% BSA solution without saponin. Images

were obtained by confocal laser scanning microscopy (Zeiss LSM 710) using a 63X oil immersion objective lens. The number of bacteria adhering per cell was calculated by dividing the total number of bacteria adhered by the total number of host cells in a single microscopic field. The counting and analysis were done with the help of ZEN Black 2009 software provided by Zeiss.

Intracellular proliferation assay

The protocol of intracellular proliferation assay has been followed as demonstrated earlier (Chaudhuri et al., 2018). Briefly, the seeded RAW264.7, U937, Caco-2, and HeLa cells (1.5 to 2 X 10^5 cells per well) were infected with STM (WT), *ΔompA*, *ΔompA*: pQE60-*ompA* and *ΔompA*:pQE60 at MOI 10, as mentioned earlier in this study. After centrifuging the cells at 800 rpm for 5 minutes, the infected cells were incubated at 37^0C temperature in presence of 5% CO_2 for 25 minutes. Next, the cells were washed thrice with PBS to remove all the unattached extracellular bacteria and subjected to 100 µg/ mL and 25 µg/ mL concentration of gentamycin treatment for 1 hour each. The cells were lysed with 0.1% triton-X-100 at 2 hours and 16 hours post-infection. The lysates were plated on *Salmonella- Shigella* Agar and the corresponding CFU at 2 hours and 16 hours were determined. The intracellular proliferation of bacteria (Fold proliferation) was determined using a simple formula-

Fold proliferation= [CFU at 16 hours]/ [CFU at 2 hours]

In some set of experiments, the fold proliferation of STM (WT) and *ΔompA* in the macrophage (RAW 264.7) was measured in the presence of iNOS inhibitor 1400W dihydrochloride [10µM] and activator mouse IFN-γ [100U/ mL]. Both inhibitor (1400W) and activator (IFN-γ) were added to the cells infected with STM (WT) and *ΔompA* along with 25 µg/ mL of gentamycin solution. As usual, the cells were lysed with 0.1% triton-X-100 at 2 hours and 16 hours post-

infection. The lysates were plated on *Salmonella- Shigella* Agar and the corresponding CFU at 2 hours and 16 hours were calculated to determine Fold proliferation.

Chloroquine resistance assay

To estimate the number of intracellular bacteria localized in the cytoplasm of macrophage and epithelial cells chloroquine resistance assay was performed using a modified protocol as described previously (Wrande et al., 2016, Knodler et al., 2014). Briefly, the seeded RAW264.7 and Caco-2 cells (density- 1.5 to 2 X 10^5 cells per well) were infected with STM- (WT), *ΔompA*, and *ΔompA*: pQE60-*ompA* at MOI 10, as mentioned earlier in this study. After centrifuging the cells at 800 rpm for 5 minutes, the infected cells were incubated at 37^0C temperature in presence of 5% CO_2 for 25 minutes. Next, the cells were washed with PBS and subjected to 100 µg/ mL and 25 µg/ mL of gentamycin treatment respectively. The old DMEM (having 25 µg/ mL gentamycin) was replaced from the wells with freshly prepared DMEM, supplemented with 25 µg/ mL gentamycin and 50 µg/ mL chloroquine two hours before lysis (14 hours post-infection). The cells were lysed with 0.1% triton-X-100 at 16 hours post-infection. The lysates were plated on *Salmonella- Shigella* agar and the corresponding CFU at 16 hours were determined. Percent abundance of cytosolic and vacuolar bacteria was obtained after dividing the CFU from chloroquine treated set with chloroquine untreated set.

Percentage of cytosolic bacteria= [CFU at 16 hours with chloroquine]/ [CFU at 16 hours without chloroquine] X 100%

Percentage of vacuolar bacteria= (100 - percentage of cytosolic bacteria) %

Confocal microscopy

For immunofluorescence study, RAW 264.7 or Caco-2 cells seeded at a density of 1.5 to 2 X 10^5 cells per sterile glass coverslip, were infected with appropriate bacterial strains at MOI 20. The cells were washed thrice with PBS and fixed with 3.5% paraformaldehyde for 15minutes

at indicated time points post-infection. The cells were first incubated with specific primary antibody raised against *Salmonella* SseC/ SseD proteins, mouse lysosome-associated membrane protein-1 (LAMP-1) (rat anti-mouse LAMP-1), mouse nitrotyrosine (mouse anti-mouse nitrotyrosine), and/or S. Typhimurium (anti- Salmonella O antigen) as per the requirements of experiments, diluted in 2.5% BSA and 0.01% saponin (dilution 1: 100, duration 6 to 8 hours at 4^0C temperature). This was followed by the incubation of the cells with appropriate secondary antibody conjugated with fluorophores (dilution 1: 200, duration 1 hours at room temperature).

The coverslips were mounted with anti-fade reagent and fixed on a glass slide with transparent nail-paint. Samples were imaged by confocal laser scanning microscopy (Zeiss LSM 710) using a 63X oil immersion objective lens. The images were analyzed with ZEN Black 2009 software provided by Zeiss.

Griess assay to measure extracellular nitrite concentration

Extracellular nitrite from infected macrophage cells was measured using a protocol described earlier (Das et al., 2009). 3.13 μM, 6.25 μM, 12.5 μM, 25 μM, 50 μM, 100 μM standard $NaNO_2$ solutions were prepared from main stock [0.1 (M) $NaNO_2$] by serial dilution in deionized distilled water. The $[OD]_{545nm}$ of the standard solutions were measured after adding and incubating them with Griess reagent and the standard curve was drawn. Culture supernatants were collected from RAW264.7 cells infected with STM- (WT), *ΔompA*, *ΔompA*: pQE60-*ompA*, *ΔompA*: pQE60, and heat-killed bacteria at 16 hours post-infection and subjected to nitrite estimation by adding Griess reagents. To 50 μL of culture supernatant, 50 μL of 1% sulphanilamide (made in 5% phosphoric acid) and 50 μL of 0.1% NED (N-1-naphthyl ethylene diamine dihydrochloride) were added and incubated for 10 minutes in darkness at room

temperature. The $[OD]_{545nm}$ was measured within 30 minutes of the appearance of a purple-colored product.

Measurement of intracellular nitric oxide

The level of intracellular nitric oxide of infected macrophage was measured using cell membrane-permeable fluorescent nitric oxide probe 4, 5- diaminofluorescein diacetate (DAF2-DA) (Lahiri et al., 2008a). Briefly, RAW264.7 cells were infected with STM- (WT), *ΔompA*, *ΔompA*: pQE60-*ompA*, *ΔompA ΔompC*, *ΔompA ΔompD*, *ΔompA ΔompF* & LLO at MOI 10 as described before. 16 hours post-infection the culture supernatants were replaced with DMEM media, supplemented with 5 µM concentration of DAF2-DA, which was followed by further incubation of the infected cells at 37^0C temperature in presence of 5% CO_2 for 30 minutes. The cells were washed with sterile PBS and acquired immediately for analysis by flow cytometry (BD FACSVerse by BD Biosciences-US) using 491 nm excitation channel and 513 nm emission channel.

Measurement of the activity of the *spiC* promoter

The activity of *spiC* promoter in STM (WT) and *ΔompA* was measured by mild alteration of a protocol described earlier (Das et al., 2009). Briefly, 1.5 mL of overnight grown stationary phase culture of STM (WT) and *ΔompA* carrying pHG86 *spiC-lacZ* construct were centrifuged at 6000 rpm for 10 minutes and the pellet was resuspended in 500 µL of Z-buffer (Na2HPO4, 60 mM; NaH2PO4, 40 mM; KCl, 10 mM; MgSO4.7H2O, 1mM). The OD of the Z-buffer was measured at 600 nm after resuspension. The cells were permeabilized by adding 5 µL of 0.1% SDS and 20 µL of chloroform and incubated at room temperature for 5 minutes. 100 µL of 4 mg/ mL of o-nitrophenyl *β*-D galactopyranoside was added in dark and incubated till the color appeared. The reaction was stopped using 250 µL 1 M Na_2CO_3. The reaction mixture was centrifuged at 6000 rpm for 10 minutes and the OD of the supernatant was measured at 420 nm

and 550 nm on a flat bottom transparent 96 well plate. STM (WT) and *ΔompA* harboring promoter-less empty pHG86 *LacZ* construct were used as control. The activity of the *spiC* promoter was measured in Miller Unit using the following formula

$$\textbf{Miller Unit (MU)} = 1000[\, OD_{420nm} - OD_{550nm} * 1.75]/\, T*V*OD_{600nm}$$

OD_{420nm}= Absorbance by o-nitrophenol and light scattering by cell debris

OD_{550nm}= light scattering by cell debris

OD_{600nm} = bacterial cell density in the washed media

T= Time of reaction in minutes

V= Volume of the culture in mL.

Measurement of the activity of the *spiC* promoter from intracellular bacteria

RAW264.7 cells were infected with STM (WT): pHG86 *spiC-LacZ* and *ΔompA*: pHG86 *spiC-LacZ* at MOI 50. After centrifuging the cells at 800 rpm for 5 minutes, the infected cells were incubated at 37^0C temperature in presence of 5% CO_2 for 25 minutes. Next, the cells were washed thrice with PBS to remove all the unattached extracellular bacteria and subjected to 100 µg/ mL and 25 µg/ mL concentration of gentamycin treatment for 1 hour each. The cells were lysed with 0.1% triton-X-100 at 12 hours post-infection. The lysates were centrifuged at 14,000 rpm for 30 minutes and the pellet was resuspended in 500 µL of Z-buffer. The OD of the Z-buffer was measured at 600 nm after resuspension. The cells were permeabilized by the addition of 5 µL of 0.1% SDS and 20 µL of chloroform and incubated at room temperature for 5 minutes. 100 µL of 4 mg/ mL of o-nitrophenyl *β*-D galactopyranoside was added in dark and incubated till the color appeared. The reaction was stopped using 250 µL 1 M Na_2CO_3. The reaction mixture was centrifuged at 6000 rpm for 10 minutes and the OD of the supernatant

was measured at 420 nm and 550 nm on a flat bottom transparent 96 well plate. The activity of the *spiC* promoter was measured in Miller Unit using the formula mentioned earlier.

Measurement of the cytosolic acidification of the bacteria using BCECF-AM

The acidification of the cytosol of the bacteria in presence of *in vitro* acidic stress was measured using a cell-permeable dual excitation ratiometric dye called 2',7'-Bis-(2-Carboxyethyl)-5-(and-6)-Carboxyfluorescein, Acetoxymethyl Ester (BCECF-AM). 4.5 X 10^7 CFU of STM (WT), *ΔompA*, and *ΔompA*: pQE60-*ompA* from 12 hours old overnight grown stationary phase culture was resuspended in phosphate buffer (of pH 5.5, 6, 6,5, and 7 respectively) separate microcentrifuge tubes and incubated for 2 hours in a shaker incubator at 37^0C temperature. 30 minutes before the flow cytometry analysis BCECF-AM (1mg/ mL) was added in each tube so that the final concentration becomes 20 µM. At the end of the incubation period of 2 hours, the bacterial cells were analyzed in flow cytometry (BD FACSVerse by BD Biosciences-US) using 405 nm and 488 nm excitation and 535 nm emission channel. The median fluorescence intensity (MFI) of the bacterial population at 488 nm and 405 nm was obtained from BD FACSuite software and the 488/ 405 ratio was determined to estimate the level of acidification of the bacterial cytosol.

Measurement of extracellular H_2O_2 by phenol red assay

H_2O_2 produced by RAW264.7 cells infected with STM- (WT), *ΔompA*, *ΔompA*: pQE60-*ompA* at MOI 10 was measured by modifying a protocol of phenol red assay as demonstrated before (Lahiri et al., 2008b). Briefly, two hours post-infection, infected RAW264.7 cells were supplemented with phenol red solution having potassium phosphate (0.01 M; pH 7.0), glucose (0.0055 M), NaCl (0.14 M), phenol red (0.2 g/ L), and HRPO (8.5 U/ mL; Sigma- Aldrich). 16 hours post-infection the culture supernatant was collected and subjected to the [OD] measurement at 610 nm wavelength in TECAN 96 well microplate reader. In presence of H_2O_2

produced by macrophage horseradish peroxidase (HRPO) converts phenol red into a compound that has enhanced absorbance at 610 nm. The concentration of H_2O_2 produced by macrophages was measured by using a standard curve of H_2O_2 in phenol red solution with known concentrations ranging from 0.5 to 5 µM.

Measurement of intracellular ROS

The level of intracellular ROS in infected macrophages was measured using membrane-permeable redox-sensitive probe 2',7'- dichlorodihydrofluorescein diacetate (H_2DCFDA) (Lahiri et al., 2008b). Upon its oxidation by intracellular esterases this non-fluorescent dye is converted into highly fluorescent 2',7'- Dichlorofluorescein (H_2DCF), which has emission at 492- 495 nm and excitation at 517 to 527 nm. Briefly, RAW264.7 cells were infected with STM- (WT), *ΔompA*, *ΔompA*: pQE60-*ompA* at MOI 10 as described before. 16 hours post-infection the culture supernatants were replaced with DMEM media, supplemented with 10 µM concentration of H_2DCFDA, which was followed by further incubation of the infected cells at 37^0C temperature in presence of 5% CO_2 for 30 minutes. The cells were washed with sterile PBS and acquired immediately for analysis by flow cytometry (BD FACSVerse by BD Biosciences-US) using 492 nm excitation channel and 517 nm emission channel.

Sensitivity assay of bacteria against *in vitro* nitrosative and oxidative stress

The sensitivity of STM (WT) and *ΔompA* was tested against *in vitro* nitrosative and oxidative stress. H_2O_2 dissolved in PBS of pH 5.4 was used for creating *in vitro* oxidative stress. Acidified nitrite ($NaNO_2$ in PBS of pH 5.4) alone and a combination of acidified nitrite along with H_2O_2 were used to generate *in vitro* nitrosative stress (Heaselgrave et al., 2010). Sensitivity was checked in both concentration and time-dependent manner.

Concentration-dependent sensitivity

10^8 CFU of overnight grown stationary phase cultures of STM- (WT) and *ΔompA* were inoculated in varying concentrations of acidified nitrite and peroxide ranging from 200 µM to 5 mM and further incubated for 12 hours. At the end of the incubation period, supernatants from each concentration were collected, serially diluted, plated on *Salmonella- Shigella* agar and the $\log_{10}$[CFU/ mL] values were acquired to determine the inhibitory concentrations of nitrite, peroxide, and both together.

Time-dependent sensitivity

10^8 CFU of overnight grown stationary phase cultures of STM- (WT) and *ΔompA* were inoculated in 800µM concentration of acidified nitrite and further incubated for 12 hours. Aliquots were collected, serially diluted, and plated on *Salmonella- Shigella* agar at 0, 3, 6, 9, 12 hours post-inoculation to monitor the CFU.

Bacterial cell viability assay by resazurin

Bacterial cell viability under the treatment of acidified nitrite and peroxide was measured using resazurin assay. Resazurin, a blue-colored non-fluorescent redox indicator is reduced into resorufin, a pink-colored fluorescent compound (having excitation at 540 nm and emission at 590 nm) by aerobic respiration of metabolically active cells. Briefly, STM- (WT) and *ΔompA* were treated with varying concentrations of acidified nitrite and peroxide as mentioned above. At the end of the incubation period, supernatants were collected and incubated with resazurin (1 µg/ mL) in a 37^0C shaker incubator at 180 rpm for 2 hours in a 96 well plate. At the end of the incubation period, the fluorescence intensity was measured using TECAN 96 well microplate reader and percent viability was calculated.

Nitrite uptake assay

Nitrite uptake by different bacterial strains [STM- (WT), *ΔompA*, *ΔompA*: pQE60-*ompA*, *ΔompA*:pQE60, *ΔompAΔompC*, *ΔompAΔompD*, *ΔompAΔompF*, *ΔompC*, *ΔompD*, *ΔompF*, and

PFA fixed dead bacteria] was determined by measuring the remaining concentration of nitrite in the uptake mixture using a protocol described earlier (Das et al., 2009). Briefly, 10^8 CFU of overnight grown stationary phase bacterial cultures were inoculated in an uptake mixture, which consists of 40 mM glucose, 80 mM MOPS-NaOH buffer (pH= 8.5), and nitrite (50/ 100/ 200 µM) in a final volume of 5 mL. The assay mixtures were kept in a 37^0C shaker incubator after the inoculation is done. At indicated time points, 150 µL of suspension from each assay mixture was collected and subjected to Griess assay to determine the level of remaining nitrite as mentioned earlier.

Examination of *in vitro* redox homeostasis of STM (WT) and *ΔompA* in response to acidified nitrite

Stationary phase cultures of STM- (WT) and *ΔompA* harboring pQE60-Grx1-roGFP2 plasmid were sub-cultured in freshly prepared 5 mL LB broth at 1: 33 ratios in presence of appropriate antibiotic in 37^0C shaker incubator at 175 rpm. Once the $[OD]_{600\ nm}$ has reached 0.3 to 0.4, 500 µM of IPTG (Sigma-Aldrich) was added and the cells were further grown in 30^0C temperature at 175 rpm for 10 to 12 hours. At the end of the incubation period, 4.5 X 10^7 CFU of bacteria were subjected to the treatment of acidified nitrite [varying concentrations (as mentioned in the figure legend) of $NaNO_2$ in PBS of pH= 5.4] for 15, 30, 45, and 60 minutes. At the end of every indicated time point, the cells were analyzed in flow cytometry (BD FACSVerse by BD Biosciences-US) using 405 nm and 488 nm excitation and 510 nm emission channel. The mean fluorescence intensity at 405 nm and 488 nm was obtained from the FITC positive (GFP expressing) population and the 405/ 488 ratio was determined.

Determination of outer membrane porosity of intracellular and extracellular bacteria by bisbenzimide

The outer membrane porosity of STM- (WT), *ΔompA*, *ΔompA*: pQE60-*ompA*, and *ΔompA*:pQE60 grown in low magnesium acidic N s medium (pH= 5.4) was measured using bisbenzimide (Sigma-Aldrich) by modifying a protocol as specified previously (Coldham et al., 2010). The bacterial strains were grown in low magnesium acidic N salt medium for 12 hours. At the end of the incubation period, the culture supernatants were collected and the $[OD]_{600\ nm}$ was adjusted to 0.1 with sterile PBS. 20 µL of bisbenzimide (10 µg/ mL) solution was added to 180 µL of culture supernatants (whose $[OD]_{600\ nm}$ has already been adjusted to 0.1) in 96 well a microplate and further incubated for 10 minutes in 37^0C shaker incubator. Because of enhanced outer membrane porosity, when bisbenzimide is taken up by the bacterial cells, it binds to the bacterial DNA and starts fluorescing. The fluorescence intensity of DNA bound bisbenzimide was measured in TECAN 96 well microplate reader using 346 nm excitation and 460 nm emission filter.

To check the outer membrane porosity of intracellular STM- (WT) and *ΔompA*, infected RAW264.7 macrophage cells were lysed with 0.1% Triton X-100. The lysate was collected and centrifuged at 300g for 5 minutes to settle down eukaryotic cell debris. The sup was collected and further centrifuged at 5000 rpm for 20 minutes to settle down the bacteria. This was followed by decanting the sup and resuspending the bacterial pellets with PBS. Finally, the suspension was subjected to bisbenzimide treatment to measure the fluorescence intensity as mentioned above.

Determination of bacterial membrane polarity using $DiBAC_4$

Outer membrane polarity of STM- (WT), *ΔompA*, *ΔompA*: pQE60-*ompA*, and *ΔompA*:pQE60 grown in low magnesium acidic N salt medium (pH= 5.4) for 12 hours was measured using a fluorescent membrane potential sensitive dye called bis-(1,3-dibutyl barbituric acid)-trimethylene oxonol (Invitrogen) (Marathe et al., 2010). Briefly, 4.5 X 10^7 CFU of each

bacterial strain was incubated with 1 µg/ml of $DiBAC_4$ for 15 minutes in a 37^0C shaker incubator. The $DiBAC_4$ treated bacterial cells were further analyzed by flow cytometry (BD FACSVerse by BD Biosciences-US) to evaluate the change in membrane polarity upon knocking out *ompA*.

Comparison of *Salmonella* Containing Vacuolar pH between WT and *ΔompA*

The SCV pH of macrophages infected with STM- (WT) and *ΔompA* was compared using a protocol reported earlier (Gogoi et al., 2018). Briefly, overnight grown stationary phase cultures of STM- (WT) and *ΔompA* were labeled with 20 µM pH rhodo red succinimidyl ester at 37^0C incubator. The cells were further washed with 0.1 (M) sodium bicarbonate buffer (pH= 8.4) post- labeling. RAW264.7 cells were infected with these labeled bacteria at MOI 50. 12 hours post-infection the cells were washed with PBS and acquired for analysis by flow cytometry (CytoFLEX by Beckman Coulter Life Sciences) using 560 nm excitation and 585 nm emission filter.

Expression profiling of *ompC, ompD, ompF* in STM- (WT), *ΔompA* and complement strains growing in LB broth, acidic N media, and macrophage

Overnight grown stationary phase cultures of STM- (WT), *ΔompA,* & *ΔompA*: pQE60-*ompA* were inoculated in freshly prepared LB broth, low magnesium acidic F media (pH= 5.4) at a ratio of 1: 100. The cells were further grown in a 37^0C shaker incubator at 180 rpm for 12 hours. RAW264.7 cells were infected with above mentioned bacterial strains at MOI 50 and incubated further for 12 hours as mentioned earlier. At the end of the specified incubation, period RNA was isolated, cDNA was synthesized and expression of *ompC, ompD, ompF* were checked as mentioned earlier.

Animal survival assay

4-6 weeks old BALB/c and C57BL/6 mice housed in the specific-pathogen-free condition of central animal facility of Indian Institute of Science, Bangalore was used for all the *in vivo* infection and survival studies. All the animal experiments were approved by the Institutional Animal Ethics Committee and the National Animal Care Guidelines were strictly followed. Two cohorts of twenty 4-6 weeks old BALB/c and C57BL/6 mice were infected with 10-12 hours old overnight grown stationary phase cultures of STM (WT) and *ΔompA* by oral gavaging at lethal dose 10^8 CFU/ animal respectively **(n= 10)**. The survival of infected mice was observed for the next few days until all the mice infected with STM (WT) died. The survival was recorded, and the data was represented as percent survival.

Determination of bacterial burden in different organs

Four cohorts of five 4-6 weeks old C57BL/6 mice were infected with STM (WT) and *ΔompA* by oral gavaging at sub-lethal dose 10^7 CFU/ animal respectively **(n= 5)**. Two of these cohorts infected with STM- (WT) and *ΔompA* strains respectively were further intraperitoneally injected with iNOS inhibitor aminoguanidine hydrochloride (AGH- 10mg/ kg of body weight) regularly for 5 days post-infection. The other two cohorts were treated with a placebo. Two cohorts of *iNOS*$^{-/-}$ mice were orally infected with STM (WT) and *ΔompA* at 10^7 CFU/ animal **(n=5)**. Two cohorts of five *gp91phox*$^{-/-}$ mice, which are unable to generate ROS were orally gavaged with STM- (WT) and *ΔompA* at 10^7 CFU/ animal **(n=5)**. On the 5th day post-infection all the mice were sacrificed, which was followed by isolation, weighing, and homogenization of specific organs like- liver, spleen, and MLN. The organ lysates were plated on *Salmonella Shigella* agar to determine the bacterial burden in different organs. The CFU corresponds to an organ was further normalized with organ weight and the $\log_{10}$[CFU/ gm-wt.] value has been plotted.

Statistical analysis

Each assay has been independently repeated 2 to 5 times [as mentioned in the figure legends]. The *in vitro* data and the results obtained from cell line experiments were analyzed by unpaired student's *t*-test and *p* values below 0.05 were considered significant. Results obtained from *in vitro* sensitivity assays were analyzed by 2way ANOVA. Data obtained from *in vivo* infection of mice were analyzed by Mann- Whitney *U* test from GraphPad Prism 8 software. Flow cytometry data were analyzed and plotted using BD FACSuite (by BD Biosciences-US) and CytoFLEX (by Beckman Coulter Life Sciences) software respectively. The results are expressed as mean ± SD or mean ± SEM. Differences between experimental groups were considered significant for $p < 0.05$.

Acknowledgments

Departmental Confocal Facility, Departmental Real-Time PCR Facility, Central Bioimaging Facility, Central Flowcytometry Facility, Department of Biochemistry Flowcytometry Facility, and Central Animal Facility at IISc are duly acknowledged. Ms. Anusha and Ms. Navya are acknowledged for their help in image acquisition. Mrs. Ranjitha is acknowledged for her help in flow cytometry data acquisition. Dr. Amit Singh (Centre for Infectious Disease Research and Department of Microbiology and Cell Biology, Indian Institute of Science, Bangalore) is acknowledged for providing pQE60-Grx1-roGFP2 construct. Ms. Debapriya Mukherjee and Ms. Dipasree Hajra are acknowledged for their timely technical support.

Funding

This work was supported by the DAE SRC fellowship (DAE00195) and DBT-IISc partnership umbrella program for advanced research in biological sciences and Bioengineering to DC Infrastructure support from ICMR (Centre for Advanced Study in Molecular Medicine), DST

(FIST), and UGC (special assistance) is acknowledged. DC acknowledges the ASTRA Chair professorship grant from IISc. ARC sincerely acknowledges IISc Fellowship from MHRD, Govt. of India, and the estate of the late Dr. Krishna S. Kaikini for the Shamrao M. Kaikini and Krishna S. Kaikini scholarship.

Availability of data and materials

All data generated and analyzed during this study, including the supplementary information files have been incorporated in this article. The data is available from the corresponding author on reasonable request.

Author Contributions

ARC and DC conceived the study and designed the experiments. ARC performed all the experiments, analyzed the data, and wrote the manuscript. SS constructed pQE60-*ompA* recombinant plasmid under the supervision of UV. SS, UV, and DC reviewed and edited the manuscript. DC supervised the study. All the authors have read and approved the manuscript.

Declarations

Ethics statement

All the animal experiments were approved by the Institutional Animal Ethics Committee and the Guidelines provided by National Animal Care were strictly followed. (Registration No: 48/1999/CPCSEA).

Consent for publication

Not applicable.

Competing interests

The authors declare that they have no conflict of interests.

Table 1. Strains and plasmids used in this study

Strains/ plasmids	Characteristics	Source/ references
Salmonella enterica serovar Typhimurium ATCC strain14028S	Wild type (WT)	Gifted by Prof. M. Hensel
S. Typhimurium *ΔompA*	Kan^R	This study
ΔompA: pQE60-*ompA*	Kan^R, Amp^R	This study
ΔompA: pQE60	Kan^R, Amp^R	This study
S. Typhimurium *ΔompC*	Chl^R	This study
S. Typhimurium *ΔompD*	Chl^R	This study
S. Typhimurium *ΔompD*	Kan^R	This study
S. Typhimurium *ΔompF*	Chl^R	This study
S. Typhimurium *ΔompA ΔompC*	Kan^R, Chl^R	This study

S. Typhimurium *ΔompA ΔompD*	Kan^R, Chl^R	This study
S. Typhimurium *ΔompA ΔompF*	Kan^R, Chl^R	This study
pKD4	Plasmid with FRT-flanked Kanamycin resistance gene	KA Datsenko & BL Wanner, PNAS, 2000
pKD46	Plasmid expressing λ red recombinase, Amp^R	KA Datsenko & BL Wanner, PNAS, 2000
pQE60 vector	Low copy number plasmid, Amp^R	Laboratory stock
pFV- mCherry (RFP)	Amp^R	Laboratory stock
pFV: GFP	Amp^R	Laboratory stock
STM (WT): *LLO*	Amp^R	Laboratory stock
STM *ΔompA*: *LLO*	Amp^R	This study
S. Typhimurium wildtype: pHG86 *spiC-LacZ*	Amp^R	This study
S. Typhimurium *ΔompA*: pHG86 *spiC-LacZ*	Amp^R	This study
pHG86 *spiC-LacZ*	Amp^R	Laboratory stock

pQE60-Grx1-roGFP2	Amp^R	Gifted by Dr. Amit Singh, CIDR, IISc

Table 2. Primer sequences (5' to 3')

ompA knockout forward-

TCGTTGGAGATATTCATGGCGTATTTTGGATGATAACGAGCATATGAATATCCTC
CTTAG

ompA knockout reverse-

AAGAAGTAACGCTGAAAGGCGTTGTCATCCAGACCAGAGCGTGTAGGCTGGAGC
TGCTTC

ompC knockout forward-

ATAACTGTAACATCTTAAAAGTTTTAGTATCATATTCGTGGTGTAGGCTGGAGCT
GCTTC

ompC knockout reverse-

TATCAAAACGTCGTATTTGTACGCCGGAATAAGGCATGATGGGAATTAGCCATG
GTCC

ompD knockout forward-

TTATTAAAATGAAACTTAAGTTAGTGGCAGTGGCAGTGTTTAAATGGCGCGCCTT
ACG

ompD knockout reverse-

CAAAATTAGAACTGGTAGTTCAGACCAACAGCAACGATGTGGAAGATCACTTCG
CAGAA

ompF knockout forward-

ATTGACGGAATTTATTGACGGCAGTGGCAGGTGTCATAGTGTAGGCTGGAGCTGC TTC

ompF knockout reverse-

TACAAAATGCCAACCGTTAGCGCTAAAAAGCCCGCCTGTTATGGGAATTAGCCA TGGTCC

ompA cloning forward- CATGCCATGGATGAAAAAGACAGCTATCGC

ompA cloning reverse- CCCAAGCTTTTGTCATCCAGACCAGAG

ompA confirmatory forward- CGGTAGAGTAACTATTGAG

ompA confirmatory reverse- TTACAGGCGTTATTAGGC

ompA expression forward- ATCCAATCACTGACGATCTG

ompA expression reverse- GCATCACCGATGTTGTTAGT

ompC confirmatory forward- GGTAAACAGACATTCAGA

ompC confirmatory reverse- AGTCATTTTCATCGCTGTT

ompD confirmatory forward- GAACTTATGCCACTCCGTCATT

ompD confirmatory reverse- CAGCATTTCGACGTCAACGGTA

ompF confirmatory forward- GTCAGACACATAAAGACACC

ompF confirmatory reverse- CGAGGTTCCATTATAGTTACAG

Kanamycin^{R} internal forward- CGGTGCCCTGAATGAACTGC

Kanamycin^{R} internal reverse- CGGCCACAGTCGATGAATCC

Chloramphenicol^{R} internal forward- ACAAACGGCATGATGAACCT

Chloramphenicol^{R} internal reverse- GCTCTGGAGTGAATACCACG

spiC expression forward- ACCTAAGCCTTGTCTTGCCT

spiC expression reverse- CCATCCGCTGTGAGCTGTAT

sseC expression forward- TTTGGCGAGGAAGTGGTTGA

sseC expression reverse- AGCCATTTCACGTTCAAGCG

sseD expression forward- TGTTGTCGGGTGTACTGACG

sseD expression reverse- ACGGCTTGACCCGCTATAAG

16srRNA forward- GAGCGCAACCCTTATCCTTTG

16srRNA forward- CACTTTATGAGGTCCGCTTGCT

References

Abreu, A.G., and Barbosa, A.S. (2017). How Escherichia coli circumvent complement-mediated killing. Frontiers in Immunology *8*, 1–6.

Balakrishnan, A., Schnare, M., and Chakravortty, D. (2016). Of men not mice: Bactericidal/permeability-increasing protein expressed in human macrophages acts as a phagocytic receptor and modulates entry and replication of gram-negative bacteria. Frontiers in Immunology *7*.

Brumell, J.H., Tang, P., Zaharik, M.L., and Finlay, B.B. (2002). Disruption of the

Salmonella-Containing Vacuole Leads to Increased Replication of Salmonella enterica Serovar Typhimurium in the Cytosol of Epithelial Cells. Infection and Immunity *70*, 3264–3270.

Calderón, I.L., Morales, E., Caro, N.J., Chahúan, C.A., Collao, B., Gil, F., Villarreal, J.M., Ipinza, F., Mora, G.C., and Saavedra, C.P. (2011). Response regulator ArcA of Salmonella enterica serovar Typhimurium downregulates expression of OmpD, a porin facilitating uptake of hydrogen peroxide. Research in Microbiology *162*, 214–222.

Canton, J., Khezri, R., Glogauer, M., and Grinstein, S. (2014). Contrasting phagosome pH regulation and maturation in human M1 and M2 macrophages. Molecular Biology of the Cell *25*, 3330–3341.

Chakraborty, S., Chaudhuri, D., and Balakrishnan, A. (2014). Salmonella methylglyoxal detoxification by STM3117 -encoded lactoylglutathione lyase affects virulence in coordination with Salmonella pathogenicity island 2 and phagosomal acidification. Microbiology *160*, 1999–2017.

Chakraborty, S., Mizusaki, H., and Kenney, L.J. (2015). A FRET-Based DNA Biosensor Tracks OmpR-Dependent Acidification of Salmonella during Macrophage Infection. PLoS Biology *13*, 1–32.

Chakravortty, D., Hansen-wester, I., and Hensel, M. (2002). Salmonella Pathogenicity Island 2 Mediates Protection of Intracellular Salmonella from Reactive Nitrogen Intermediates. Journal of Experimental Medicine *195*, 1155–1166.

Chakravortty, D., Rohde, M., Jäger, L., Deiwick, J., and Hensel, M. (2005). Formation of a novel surface structure encoded by Salmonella Pathogenicity Island 2. EMBO Journal *24*, 2043–2052.

Chaudhuri, D., Chowdhury, A.R., and Biswas, B. (2018). Salmonella Typhimurium Infection Leads to Colonization of the Mouse Brain and Is Not Completely Cured With Antibiotics. Frontiers in Microbiology *9*, 1–12.

Choi, U., and Lee, C. (2019). Distinct Roles of Outer Membrane Porins in Antibiotic Resistance and Membrane Integrity in Escherichia coli. Frontiers in Microbiology *10*, 1–9.

Coldham, N.G., Webber, M., Woodward, M.J., and Piddock, L.J.V. (2010). A 96-well plate fluorescence assay for assessment of cellular permeability and active efflux in Salmonella enterica serovar Typhimurium and Escherichia coli. Journal of Antimicrobial Chemotherapy *65*, 1655–1663.

Collaborators, G. 2017 T. and P. (2019). The global burden of typhoid and paratyphoid fevers : a systematic analysis for the Global Burden of Disease Study 2017. The Lancet Infectious Diseases *3099*, 369–381.

Das, P., Lahiri, A., Lahiri, A., and Chakravortty, D. (2009). Novel role of the nitrite transporter NirC in Salmonella pathogenesis : SPI2-dependent suppression of inducible nitric oxide synthase in activated macrophages. Microbiology *155*, 2476–2489.

Datsenko, K.A., and Wanner, B.L. (2000). One-step inactivation of chromosomal genes in Escherichia coli K-12 using PCR products. Proceedings of the National Academy of Sciences of the United States of America *97*, 6640–6645.

Deiwick, J., Nikolaus, T., Erdogan, S., and Hensel, M. (1999). Environmental regulation of Salmonella pathogenicity island 2 gene expression. Molecular Microbiology *31*, 1759–1773.

Ebbensgaard, A., Mordhorst, H., Aarestrup, F.M., and Hansen, E.B. (2018). The Role of Outer Membrane Proteins and Lipopolysaccharides for the Sensitivity of Escherichia coli to Antimicrobial Peptides. Frontiers in Microbiology *9*, 1–13.

Eriksson, S., Lucchini, S., Thompson, A., Rhen, M., and Hinton, J.C.D. (2003). Unravelling the biology of macrophage infection by gene expression profiling of intracellular Salmonella enterica. Molecular Microbiology *47*, 103–118.

Fang, F.. Perspectives Series : Host / Pathogen Interactions. Journal of Clinical Investigation *99*, 2818–2825.

Foster, N., Hulme, S.D., Barrow, P.A., Al, F.E.T., and Mmun, I.N.I. (2003). Induction of Antimicrobial Pathways during Early-Phase Immune Response to Salmonella spp . in Murine Macrophages : Gamma Interferon (IFN- γ) and Upregulation of IFN- γ Receptor Alpha Expression Are Required for NADPH Phagocytic Oxidase gp91-Stimulated O. Infection and Immunity *71*, 4733–4741.

Galan, J.E. (2001). SALMONELLA INTERACTIONS WITH HOST CELLS : Type III Secretion at Work. Annual Review of Cell and Developmental Biology *17*, 53–86.

Gallois, A., Klein, J.R., Allen, L.-A.H., Jones, B.D., and Nauseef, W.M. (2001). Salmonella Pathogenicity Island 2-Encoded Type III Secretion System Mediates Exclusion of NADPH Oxidase Assembly from the Phagosomal Membrane . The Journal of Immunology *166*, 5741–5748.

Garai, P., Gnanadhas, D.P., and Chakravortty, D. (2012). Salmonella enterica serovars Typhimurium and Typhi as model organisms Revealing paradigm of host-pathogen interactions. VIRULENCE *3*, 377–388.

Garai, P., Lahiri, A., Ghosh, D., and Chatterjee, J. (2016). Peptide-utilizing carbon starvation gene yjiY is required for flagella-mediated infection caused by Salmonella. Microbiology *162*, 100–116.

Ghai, I., and Ghai, S. (2018). Understanding antibiotic resistance via outer membrane

permeability. Infection and Drug Resistance *11*, 523–530.

Gogoi, M., Ravikumar, V., Dixit, N.M., and Chakravortty, D. (2018). Salmonella escapes antigen presentation through K63 ubiquitination mediated endosomal proteolysis of MHC II via modulation of endosomal acidification in dendritic cells. Pathogens and Disease *76*, 1–16.

Gogoi, M., Shreenivas, M.M., and Chakravortty, D. (2019). Hoodwinking the Big-Eater to Prosper: The Salmonella -Macrophage Paradigm. Journal of Innate Immunity *11*, 289–299.

Hans Reuter, W., Masuch, T., Ke, N., Lenon, M., Radzinski, M., Loi Van, V., Ren, G., Riggs, P., Antelmann, H., Reichmann, D., et al. (2019). Utilizing redox-sensitive GFP fusions to detect in vivo redox changes in a genetically engineered prokaryote. Redox Biology *26*, 101280.

Haraga, A., Ohlson, M.B., and Miller, S.I. (2008). Salmonellae interplay with host cells. *6*, 53–66.

Hautefort, I., Thompson, A., Parker, M.L., Lucchini, S., Danino, V., Bongaerts, R.J.M., Ahmad, N., Rhen, M., and Hinton, J.C.D. (2008). During infection of epithelial cells Salmonella enterica serovar Typhimurium undergoes a time-dependent transcriptional adaptation that results in simultaneous expression of three type 3 secretion systems. Cellular Microbiology *10*, 958–984.

Heaselgrave, W., Andrew, P.W., and Kilvington, S. (2010). Acidified nitrite enhances hydrogen peroxide disinfection of Acanthamoeba, bacteria and fungi. Journal of Antimicrobial Chemotherapy *65*, 1207–1214.

Heijden, J. Van Der, Bosman, E.S., Reynolds, L.A., and Finlay, B.B. (2015). Direct measurement of oxidative and nitrosative stress dynamics in Salmonella inside macrophages. Proceedings of the National Academy of Sciences of the United States of America *112*, 560–

565.

Heijden, J. Van Der, Reynolds, L.A., Deng, W., Mills, A., Scholz, R., Imami, K., Foster, L.J., Duong, F., and Finley, B.B. (2016). Salmonella Rapidly Regulates Membrane Permeability To Survive Oxidative Stress. MBio *7*, 1–11.

Hejair, H.M.A., Zhu, Y., Ma, J., Zhang, Y., Pan, Z., Zhang, W., and Yao, H. (2017). Functional role of ompF and ompC porins in pathogenesis of avian pathogenic Escherichia coli. Microbial Pathogenesis *107*, 29–37.

Hölzer, S.U., and Hensel, M. (2010). Functional dissection of translocon proteins of the Salmonella Pathogenicity Island 2-encoded type III secretion system. BMC Microbiology *10*.

Ipinza, F., Collao, B., Monsalva, D., Bustamante, V.H., Luraschi, R., Alegría-Arcos, M., Almonacid, D.E., Aguayo, D., Calderón, I.L., Gil, F., et al. (2014). Participation of the Salmonella OmpD porin in the infection of RAW264.7 macrophages and BALB/c mice. PLoS ONE *9*.

Iyer, R., Moussa, S.H., Durand-Réville, T.F., Tommasi, R., and Miller, A. (2018). Acinetobacter baumannii OmpA Is a Selective Antibiotic Permeant Porin. ACS Infectious Diseases *4*, 373–381.

Knodler, L.A., Nair, V., and Steele-mortimer, O. (2014). Quantitative Assessment of Cytosolic Salmonella in Epithelial Cells. PLoS ONE *9*.

Knuff, K., and Finlay, B.B. (2017). What the SIF Is Happening — The Role of Intracellular Salmonella -Induced Filaments. Frontiers in Cellular and Infection Microbiology *7*, 1–8.

Kono, Y., Shibata, H., Adachi, K., Tanaka, K. Lactate-Dependent Killing of Escherichia coli by Nitrite plus Hydrogen-Peroxide: A Possible Role of Nitrogen Dioxide. Archives of Biochemistry and Biophysics *311*, 153–159.

Krishnan, S., and Prasadarao, N. V. (2012). Outer membrane protein A and OprF: Versatile roles in Gram-negative bacterial infections. FEBS Journal *279*, 919–931.

Kukkonen, M., and Korhonen, T.K. (2004). The omptin family of enterobacterial surface proteases/adhesins: from housekeeping in Escherichia coli to systemic spread of Yersinia pestis. International Journal of Medical Microbiology *294*, 7–14.

Lahiri, A., Das, P., and Chakravortty, D. (2008a). Arginase modulates Salmonella induced nitric oxide production in RAW264 . 7 macrophages and is required for Salmonella pathogenesis in mice model of infection. Microbes and Infection *10*, 1166–1174.

Lahiri, A., Das, P., and Chakravortty, D. (2008b). The LysR-type transcriptional regulator Hrg counteracts phagocyte oxidative burst and imparts survival advantage to Salmonella enterica serovar Typhimurium. Microbiology *154*, 2837–2846.

Li, W., Wen, L., Li, C., Chen, R., Ye, Z., Zhao, J., and Pan, J. (2016). Contribution of the outer membrane protein OmpW in Escherichia coli to complement resistance from binding to factor H. Microbial Pathogenesis *98*, 57–62.

Marathe, S.A., Ray, S., and Chakravortty, D. (2010). Curcumin Increases the Pathogenicity of Salmonella enterica Serovar Typhimurium in Murine Model. PLoS ONE *5*.

March, C., Moranta, D., Regueiro, V., Llobet, E., Tomás, A., Garmendia, J., and Bengoechea, J. (2011). Klebsiella pneumoniae outer membrane protein A is required to prevent the activation of airway epithelial cells. Journal of Biological Chemistry *286*, 9956–9967.

Mittal, R., Krishnan, S., Gonzalez-Gomez, I., and Prasadarao, N. V. (2011). Deciphering the roles of outer membrane protein A extracellular loops in the pathogenesis of Escherichia coli K1 meningitis. Journal of Biological Chemistry *286*, 2183–2193.

Mohan Nair, M.K., and Venkitanarayanan, K. (2007). Role of bacterial OmpA and host

cytoskeleton in the invasion of human intestinal epithelial cells by Enterobacter sakazakii. Pediatric Research *62*, 664–669.

Nevermann, J., Silva, A., Otero, C., Oyarzún, D.P., Barrera, B., Gil, F., Calderón, I.L., and Fuentes, J.A. (2019). Identification of genes involved in biogenesis of Outer Membrane Vesicles (OMVs) in Salmonella enterica Serovar Typhi. Frontiers in Microbiology *10*, 1–17.

Panday, A., Sahoo, M.K., Osorio, D., and Batra, S. (2015). NADPH oxidases: An overview from structure to innate immunity-associated pathologies. Cellular and Molecular Immunology *12*, 5–23.

Park, J.S., Lee, W.C., Yeo, K.J., Ryu, K.-S., Kumarasiri, M., Hesek, D., Lee, M., Mobashery, S., Song, J.H., Kim, S. Il, et al. (2012). Mechanism of anchoring of OmpA protein to the cell wall peptidoglycan of the gram-negative bacterial outer membrane. The FASEB Journal *26*, 219–228.

Pearse, D.D., Chatzipanteli, K., Marcillo, A.E., Bunge, M.B., and Dietrich, W.D. (2003). Comparison of iNOS Inhibition by Antisense and Pharmacological Inhibitors after Spinal Cord Injury. Journal of Neuropathology and Experimental Neurology *62*, 1096–1107.

Ruan, Y., Rezelj, S., Bedina Zavec, A., Anderluh, G., and Scheuring, S. (2016). Listeriolysin O Membrane Damaging Activity Involves Arc Formation and Lineaction – Implication for Listeria monocytogenes Escape from Phagocytic Vacuole. PLoS Pathogens *12*, 1–18.

Rychlik, I., and Barrow, P.A. (2005). Salmonella stress management and its relevance to behaviour during intestinal colonisation and infection. FEMS Microbiology Reviews *29*, 1021–1040.

Salcedo, S.P., Holden, D.W., and Beuzo, C.R. (2002). Growth and killing of a Salmonella enterica serovar Typhimurium sifA mutant strain in the cytosol of different host cell lines.

Microbiology *148*, 2705–2715.

Singamsetty, V.K., Wang, Y., Shimada, H., and Prasadarao, N. V. (2008). Outer membrane protein A expression in Enterobacter sakazakii is required to induce microtubule condensation in human brain microvascular endothelial cells for invasion. Microbial Pathogenesis *45*, 181–191.

Smani, Y., Fàbrega, A., Roca, I., Sańchez-Encinales, V., Vila, J., and Pachón, J. (2014). Role of OmpA in the multidrug resistance phenotype of Acinetobacter baumannii. Antimicrobial Agents and Chemotherapy *58*, 1806–1808.

Sukumaran, S.K., Shimada, H., and Prasadarao, N. V. (2003). Entry and intracellular replication of Escherichia coli K1 in macrophages require expression of outer membrane protein A. Infection and Immunity *71*, 5951–5961.

Tung Ngoc, Q., Linzer, N., Loi Van, V., and Antelmann, H. (2018). Application of genetically encoded redox biosensors to measure dynamic changes in the glutathione, bacillithiol and mycothiol redox potentials in pathogenic bacteria. Free Radical Biology and Medicine *128*, 84–96.

Uchiya, K.I., and Nikai, T. (2005). Salmonella pathogenicity island 2-dependent expression of suppressor of cytokine signaling 3 in macrophages. Infection and Immunity *73*, 5587–5594.

Uchiya, K.I., and Nikai, T. (2008). Salmonella virulence factor SpiC is involved in expression of flagellin protein and mediates activation of the signal transduction pathways in macrophages. Microbiology *154*, 3491–3502.

Umezawa, K., Akaike, T., Fujii, S., Suga, M., Setoguchi, K., Ozawa, A., and Maeda, H. (1997). Induction of Nitric Oxide Synthesis and Xanthine Oxidase and Their Roles in the

Antimicrobial Mechanism against Salmonella typhimurium Infection in Mice. Infection and Immunity *65*, 2932–2940.

Vergalli, J., Bodrenko, I. V., Masi, M., Moynié, L., Acosta-Gutiérrez, S., Naismith, J.H., Davin-Regli, A., Ceccarelli, M., van den Berg, B., Winterhalter, M., et al. (2020). Porins and small-molecule translocation across the outer membrane of Gram-negative bacteria. Nature Reviews Microbiology *18*, 164–176.

Vlahos R, Stambas J, Bozinovski S, Broughton BRS, Drummond GR, S.S. (2011). Inhibition of Nox2 Oxidase Activity Ameliorates Influenza A Virus-Induced Lung Inflammation. PLoS Pathogens *7(2)*, 1–11.

Webb, J.L., Harvey, M.W., Holden, D.W., and Evans, T.J. (2001). Macrophage nitric oxide synthase associates with cortical actin but is not recruited to phagosomes. Infection and Immunity *69*, 6391–6400.

Weller, R., Price, R.J., Ormerod, A.D., Benjamin, N., and Leifert, C. (2001). Antimicrobial effect of acidified nitrite on dermatophyte fungi , Candida and bacterial skin pathogens. Journal of Applied Microbiology *90*, 648–652.

Wrande, M., Andrews-polymenis, H., Twedt, D.J., Steele-mortimer, O., Porwollik, S., Mcclelland, M., and Knodler, L.A. (2016). Genetic Determinants of Salmonella enterica Serovar Typhimurium Proliferation in the Cytosol of Epithelial Cells. Infection and Immunity *84*, 3517–3526.

Wu, X., Tian, L., Zou, H., Wang, C., Yu, Z., Tang, C., Zhao, F., and Pan, J. (2013). Outer membrane protein OmpW of Escherichia coli is required for resistance to phagocytosis. Research in Microbiology *164*, 848–855.

Zielonka, J., Zielonka, M., Verplank, L., Cheng, G., Hardy, M., Ouari, O., Ayhan, M.M.,

Podsiadły, R., Sikora, A., Lambeth, J.D., et al. (2016). Mitigation of NADPH Oxidase 2 Activity as a Strategy to Inhibit Peroxynitrite Formation *. THE JOURNAL OF BIOLOGICAL CHEMISTRY *291*, 7029–7044.

Figure Legends

Figure 1.

OmpA promotes the evasion of phagocytosis and intracellular survival of *Salmonella* in macrophages.

(A) RAW 264.7 cells and PMA activated U937 cells were infected with STM wild type (WT), *ΔompA*, *ΔompA*: pQE60-*ompA*, & *ΔompA*: pQE60 respectively at MOI 10. 2 hours post-infection the cells were lysed and plated. The CFU at 2 hours was normalized with pre-inoculum to calculate the percent phagocytosis, (n=3, N=3). (B) RAW 264.7 cells were infected with STM- (WT), *ΔompA*, *ΔompA*: pQE60-*ompA*, & *ΔompA*: pQE60 respectively at MOI 50. Cells were fixed at 15 minutes post-infection with PFA. Externally attached bacteria were probed with anti-*Salmonella* antibody without saponin. 20 microscopic fields were analyzed to calculate the no. of adherent bacteria/ total no. of cells per field. Scale bar = 20μm, (n=20, N=3). (C) RAW264.7 cells and PMA activated U937 cells were infected with STM- (WT), *ΔompA*, *ΔompA*: pQE60-*ompA*, & *ΔompA*: pQE60 respectively at MOI 10. 16- and 2-hours post-infection the cells were lysed and plated. The CFU at 16 hours were normalized with the CFU at 2 hours to calculate the fold proliferation of bacteria in macrophage, (n=3, N=3). (D) RAW264.7 cells were infected with STM- (WT): RFP, *ΔompA*: RFP, *ΔompA*: pQE60-*ompA* at MOI of 20. PFA fixed wild-type bacteria was used for infection at MOI 25. Cells were fixed at 16 hours post-infection & LAMP-1 was labeled with anti-mouse LAMP-1 antibody. To stain the complemented strain and PFA fixed dead bacteria anti-*Salmonella*

antibody was used. The quantification of LAMP-1 recruitment on bacteria in RAW 264.7 cells has been represented in form of a graph. Percent colocalization was determined after analyzing 50 different microscopic fields from three independent experiments. Scale bar = 5μm, (n=50, N=3). (E) Chloroquine resistance assay of RAW 264.7 cells infected with STM- (WT), *ΔompA*, *ΔompA*: pQE60-*ompA* strains respectively, (n=3, N=2).

(P)* *< 0.05, *(P)* **< 0.005, *(P)* ***< 0.0005, *(P)* *< 0.0001, ns= non-significant, (Student's *t*-test).**

Figure 2.

OmpA dependent protection of *Salmonella* against nitrosative stress inside RAW264.7 cells.

(A) Estimation of extracellular nitrite from the culture supernatant of RAW264.7 cells infected with STM- (WT), *ΔompA*, *ΔompA*: pQE60-*ompA*, *ΔompA*: pQE60, & heat-killed bacteria respectively at MOI 10. 16 hours post-infection the culture supernatants were collected and subjected to Griess assay, (n=3, N=5). (B) Estimation of the level of intracellular nitric oxide in RAW 264.7 cells infected with STM- (WT), *ΔompA*, and *ΔompA*: pQE60-*ompA* at MOI 10, 16 hours post-infection using DAF-2 DA [5 μM] by flow cytometry. Unstained and uninfected RAW264.7 cells have also been used as controls. Both dot plots (SSC-A vs DAF-2 DA) and histograms (Count vs DAF-2 DA) have been represented. The percent population of DAF-2 DA positive RAW264.7 cells has been represented in form of a graph, (n=3, N=3). (C) Immunofluorescence image of RAW264.7 cells infected with STM- (WT): RFP, *ΔompA*: RFP, (WT): *LLO*, and *ΔompA*: *LLO* at MOI 20. 16 hours post-infection the cells were fixed with PFA and labeled with anti-*Salmonella* antibody and anti-mouse nitrotyrosine antibody followed by visualization under confocal microscopy. Percent colocalization of STM- (WT), *ΔompA*, (WT): *LLO*, and *ΔompA*: *LLO* with nitrotyrosine was determined by analyzing 50

different microscopic fields from three independent experiments, (n=50, N=3). Scale bar = 5µm. (D) RAW264.7 cells were infected with STM- (WT), *ΔompA* & (WT): *LLO* at MOI 10. 16- and 2-hours post-infection the cells were lysed and plated. The CFU at 16 hours were normalized with the CFU at 2 hours to calculate the fold proliferation of bacteria, (n=3, N=3). (E) The transcript-level expression profile of *spiC* from RAW264.7 cells infected with STM- (WT), *ΔompA* & (WT): *LLO* at MOI 50. STM (WT) infected RAW264.7 cells treated with bafilomycin A (50 nM) was used as a control. 12 hours post-infection the cells were lysed, and total RNA was extracted. After the synthesis of cDNA, the expression of *spiC* was measured by RT PCR, (n=3, N=3). (F) The measurement of the activity of *spiC* promoter in stationary phase culture of STM- (WT) and *ΔompA* growing overnight in LB media, (n=6, N=2). The measurement of the activity of *spiC* promoter in STM- (WT) and *ΔompA* proliferating intracellularly in RAW264.7 cells (MOI= 50) 12 hours post-infection. Macrophage infected with STM- (WT) and further treated with bafilomycin A (50 nM) has been used as a negative control, (n=5, N=2). (G) Estimation of intracellular acidification of STM- (WT), *ΔompA*, and *ΔompA*: pQE60-*ompA* in phosphate buffer of pH 5.5, 6, 6.5, and 7 respectively using 20 µM of ratiometric pH indicator BCECF-AM by flow cytometry. The ratio of median fluorescence intensity of BCECF-AM labeled on STM- (WT), *ΔompA*, and *ΔompA*: pQE60-*ompA* at 488 and 405 nm respectively, (n=4, N=3).

(P)* *< 0.05, *(P)* **< 0.005, *(P)* ***< 0.0005, *(P)* *< 0.0001, ns= non-significant, (Student's *t* test).**

Figure 3.

Alteration in the activity of iNOS by using specific inhibitor or activator changes the fate of STM *ΔompA* in *in vitro* and *in vivo* infection model.

Intracellular survival of STM- (WT) and *ΔompA* (MOI-10) in RAW264.7 cells (16 hours post-infection) in presence and absence of iNOS (A) inhibitor- 1400W dihydrochloride [10 µM] and (B) activator- mouse IFN-ɣ [100U/ mL]. Fold proliferation of bacteria was calculated by normalizing the CFU at 16 hours to CFU at 2 hours, (n=3, N=3). (C) Immunofluorescence image of RAW264.7 cells infected with STM- (WT) and *ΔompA* (MOI=20) in presence and absence of iNOS inhibitor- 1400W dihydrochloride [10 µM] and activator- mouse IFN-ɣ [100U/ mL]. 16 hours post-infection the cells were fixed with PFA and probed with anti-*Salmonella* antibody and anti-mouse nitrotyrosine antibody. The quantification of the recruitment of nitrotyrosine on STM- (WT) and *ΔompA* (MOI-20) in RAW264.7 cells (16 hours post-infection) in presence and absence of iNOS (D) inhibitor- 1400W dihydrochloride [10 µM] and (E) activator- mouse IFN-ɣ [100U/ mL]. Percent colocalization of bacteria with nitrotyrosine was determined after analyzing more than 50 different microscopic fields from two independent experiments, (n≥ 50, N=2). (F) The schematic representation of the strategy of animal experiment. (G) Four cohorts of 4 to 6 weeks old five C57BL/6 mice were orally gavaged with STM- (WT) and *ΔompA* at a sublethal dose of 10^7 CFU/ animal. Two of these four cohorts were intraperitoneally injected with iNOS inhibitor aminoguanidine hydrochloride (10mg/ kg of body weight) regularly for 5 days post-infection. Two cohorts of five *iNOS*$^{-/-}$ and *gp91phox*$^{-/-}$ mice were orally gavaged with STM- (WT) and *ΔompA* at a sublethal dose of 10^7 CFU/ animal separately. On the 5th-day post-infection, the mice were sacrificed, which was followed by isolation, homogenization of liver, spleen, and MLN. The organ lysates were plated on *Salmonella Shigella* agar. The colonies were counted 16 hours post-plating. The $\log_{10}$[CFU/ gm-wt.] for each CFU has been plotted, (n=5, N=3). (H) Two cohorts- each consisting of 4 to 6 weeks old 20- BALB/c and C57BL/6 mice infected with a lethal dose (10^8 CFU/ animal) of STM- (WT) and *ΔompA*. After they were infected by oral gavaging, the survival of the mice was monitored till the death of all the wild type infected mice, (n=10).

(P)* *< 0.05, *(P)* **< 0.005, *(P)* ***< 0.0005, *(P)* *< 0.0001, ns= non-significant, (Student's *t* test, Mann-Whitney *U* test- for animal survival).**

Figure 4.

OmpA dependent regulation of outer membrane permeability in *Salmonella* controls cytoplasmic redox homeostasis in response to *in vitro* nitrosative stress.

(A) Time-dependent *in vitro* death kinetics of STM- (WT) and *ΔompA* in presence of acidified nitrite (Nitrite concentration 800 µM in PBS of pH 5.4). 10^8 CFU of overnight grown stationary phase culture of both the strains were inoculated in acidified nitrite. The survival of both the strains was determined by plating the supernatant with appropriate dilution in SS agar plates at 0, 3, 6, 9, 12 hours post-inoculation, (N=5). (B) *In vitro* nitrite uptake assay of STM- (WT), *ΔompA*, *ΔompA*: pQE60-*ompA*, *ΔompA*: pQE60, & PFA fixed dead bacteria. 10^8 CFU of overnight grown stationary phase culture of all the strains were inoculated in MOPS- NaOH buffer (pH= 8.5) with an initial nitrite concentration of 200 µM. The remaining nitrite concentration of the media was determined by Griess assay at 0, 3, 6, 9, 12 hours post-inoculation, (n=3, N=4). (C) Measurement of redox homeostasis of STM- (WT) and *ΔompA* harboring pQE60-Grx1-roGFP2 in response to varying concentrations of acidified nitrite in a time-dependent manner. 4.5X 10^7 CFU of overnight grown stationary phase culture of STM (WT) and *ΔompA* expressing pQE60-Grx1-roGFP2 were subjected to the treatment of acidified nitrite (concentration of 800µM, 1mM, 5mM) for 15, 30, 45, and 60 minutes. Median fluorescence intensities of Grx1-roGFP2 at 405nm and 488nm for FITC positive population were used to obtain the 405/ 488 ratio in 800 µM, 1mM, 5 mM concentration of acidified nitrite respectively, (n=3, N=3). (D) The transcript level expression profiling of larger porin genes namely- *OmpC*, *OmpD*, *OmpF* by real-time PCR in STM- (WT), *ΔompA*, & *ΔompA*: pQE60-*ompA* in nutritionally enriched LB media, low magnesium acidic F media (pH= 5.4) mimicking the internal environment of *Salmonella* containing vacuole, and RAW264.7 murine

macrophage cells (MOI 50), [12 hours post inoculation], (n=3, N=2). (E) Measurement of membrane porosity of STM- (WT), *ΔompA*, *ΔompA*: pQE60-*ompA*, & *ΔompA*: pQE60 in acidic F media [12 hours post inoculation] using a slightly negatively charged dye named $DiBAC_4$ (final concentration- 1 µg/ mL) by flow cytometry. Unstained bacterial cells were used as control. Both dot plots (SSC-A vs $DiBAC_4$) and histograms (Count vs $DiBAC_4$) have been represented. The median fluorescence intensity of $DiBAC_4$ has been represented here, (n=3, N=2). (F) Measurement of outer membrane porosity of STM- (WT), *ΔompA*, *ΔompA*: pQE60-*ompA* & *ΔompA*: pQE60 in acidic F media [12 hours post inoculation] using a nuclear binding fluorescent dye bisbenzimide [excitation- 346 nm and emission- 460 nm] (final concentration- 1 µg/ mL). (WT) treated with 0.1% saponin for 15 minutes has been used as a positive control, (n=8, N=3). (G) Measurement of outer membrane porosity of STM- (WT) and *ΔompA* isolated from infected RAW264.7 cells 12 hours post-infection by bisbenzimide (Sigma) (final concentration- 1 µg/ mL), (n=6, N=3).

(P)* *< 0.05, *(P)* **< 0.005, *(P)* ***< 0.0005, *(P)* *< 0.0001, ns= non-significant, (2way ANOVA, Student's *t*-test).**

Figure 5.

The maintenance of the integrity of the SCV membrane inside RAW264.7 macrophage solely depends upon OmpA, not on other larger porins such as OmpC, OmpD, and OmpF.

(A) RAW264.7 cells were infected with STM- (WT), *ΔompA*, *ΔompAΔompC*, *ΔompAΔompD*, *ΔompAΔompF*, & WT: *LLO* at MOI 20. Cells were fixed at 16 hours post-infection, followed by labeled with anti-*Salmonella* antibody and anti-mouse LAMP-1 antibody. (B) Quantification of LAMP-1 recruitment on STM- (WT), *ΔompA*, *ΔompAΔompC*, *ΔompAΔompD*, *ΔompAΔompF*, (WT): *LLO*. Percent colocalization between bacteria and

LAMP-1 was determined after analyzing more than 50 different microscopic fields from two independent experiments, (n≥50, N=2). Scale bar = 5μm. (C) RAW264.7 cells were infected with STM- (WT), *ΔompA*, *ΔompC*, *ΔompD*, and *ΔompF* at MOI 20. Cells were fixed at 16 hours post-infection, followed by labeled with anti-*Salmonella* antibody and anti-mouse LAMP-1 antibody respectively. (D) Quantification of LAMP-1 recruitment on STM- (WT), *ΔompA*, *ΔompC*, *ΔompD*, and *ΔompF*. Percent colocalization of bacteria with LAMP-1 has been determined after analyzing more than 60 different microscopic fields from two independent experiments, (n≥60, N=2). Scale bar = 5μm.

(P)* *< 0.0001, (Student's *t* test).**

Figure 6.

In absence of OmpA, porins OmpC and OmpF enhance the susceptibility of *Salmonella* against the nitrosative stress of RAW264.7 cells.

(A) *In vitro* nitrite uptake assay of STM- (WT), *ΔompA*, *ΔompAΔompC*, *ΔompAΔompD*, *ΔompAΔompF*, & PFA fixed dead bacteria. 10^8 CFU of overnight grown stationary phase culture of all the strains were inoculated in MOPS- NaOH buffer (pH= 8.5) with 100 μM initial concentration of nitrite. The remaining nitrite in the media was estimated by Griess assay at 0, 2, 4, 6, 8 hours post-inoculation, (n=3, N=6). (B) *In vitro* viability assay of STM- (WT), *ΔompA*, *ΔompAΔompC*, *ΔompAΔompD*, & *ΔompAΔompF* in presence of acidified nitrite [800 μM] 12 hours post-inoculation using resazurin solution, (n=3, N=3). (C) Immunofluorescence image of RAW264.7 cells infected with STM- (WT), *ΔompA*, *ΔompAΔompC*, *ΔompAΔompD*, *ΔompAΔompF*, & (WT): *LLO* at MOI 20. Cells were fixed at 16 hours post-infection, followed by labeled with anti-*Salmonella* antibody and anti-mouse nitrotyrosine antibody. Quantification of nitrotyrosine recruitment on STM- (WT), *ΔompA*, *ΔompAΔompC*, *ΔompAΔompD*, *ΔompAΔompF*, (WT): *LLO* has been represented in form of a graph. Percent

colocalization between bacteria and nitrotyrosine was determined after analyzing more than 60 different microscopic fields from two independent experiments, (n≥60, N=3). Scale bar = 5µm. (D) Intracellular survival of STM- (WT), *ΔompA*, *ΔompAΔompC*, *ΔompAΔompD*, & *ΔompAΔompF*, & (WT): *LLO* respectively (MOI 10) in RAW264.7 cells. 16- and 2-hours post-infection the cells were lysed and plated. The CFU at 16 hours were normalized with the CFU at 2 hours to calculate the fold proliferation of bacteria in macrophage, (n=3, N=3). (E) Estimation of the intracellular nitrite level in RAW 264.7 cells infected with STM- (WT), *ΔompA*, *ΔompAΔompC*, *ΔompAΔompD*, *ΔompAΔompF*, and (WT): *LLO* respectively at MOI 10, 16 hours post-infection using DAF-2 DA [5 µM] by flow cytometry. Unstained cells have also been used as control. Both dot plots (SSC-A vs DAF-2 DA) and histograms (Count vs DAF-2 DA) have been represented. Median fluorescence intensity of DAF-2 DA has been represented in form of a graph, (n=3, N=3).

(P)* *< 0.05, *(P)* **< 0.005, *(P)* ***< 0.0005, *(P)* *< 0.0001, ns= non-significant, (Student's *t* test).**

Figure 7.

The hypothetical model that depicts the fate of (A) STM (WT), (B) STM *ΔompA*, and (C) STM (WT): *LLO* inside the murine macrophage. (A) STM (WT) staying inside the acidic SCV can proliferate efficiently by suppressing the activity of iNOS in SpiC dependent manner, (B) STM *ΔompA*, which is unable to remain in SCV, is heavily bombarded with RNI in the cytosol of macrophage, (C) STM (WT): *LLO* can survive in the cytosol by reducing its outer membrane permeability to RNI with the help of OmpA.

Figure S1.

OmpA plays a crucial role in the survival of *Salmonella* Typhimurium in murine macrophage.

The transcript level expression profile of (A) *ompA*, (C) *ompC*, (E) *ompD*, and (G) *ompF* in STM- (WT) at indicated time points (3, 6, 9, 12 hours) in LB broth (n=3, N=3), low magnesium acidic F media (pH=5.4) (n=3, N=3), and RAW264.7 murine macrophage cells (MOI= 50), (n=3, N=3). The predicted structures of (A) OmpA, (B) OmpC, (C) OmpD, and (D) OmpF using SWISS-MODEL protein structure homology-modeling server.

***(P)* *< 0.05, *(P)* **< 0.005, (Student's *t* test).**

Figure S2.

STM *ompA* knockout and complement strains generation, confirmation and analysis of growth kinetics in LB media

(A) Confirmation of *ompA* knockout in *Salmonella* using confirmatory primers, [Colonies C-2, 3, 5, 6, 7, 9, 10, 12, 13 are *ompA* knockout (1.7kb size), W- STM (WT) (1.3 kb size)] (B) Confirmation of knockout using kanamycin internal primers (Kan^R) [Colonies C-1, 2, 3, 4, 5, 6, 7, 8, 9, 10, 11, 12, 13 are *ompA* knock out (.47 kb size), W- STM WT (no band)], (C) Confirmation of complement strain generation by restriction digestion [DD- Double digested plasmid , SD1, SD2- Single digested plasmid, NC- Negative Control (No Enzyme), UC- Uncut plasmid, L- Ladder], (D) Confirmation of *ompA* knockout and complementation strain by RT PCR, (n=4, N=2), (E-F) Growth kinetics of STM (WT), STM *ΔompA,* STM *ΔompA*: pQE60-*ompA,* STM *ΔompA*: pQE60 in (E) $[OD]_{600nm}$ and (F) log_{10}[CFU/mL] respectively, (n=3, N=3).
(P)* *< 0.05, *(P)* **< 0.005, *(P)* *< 0.0001, ns= non-significant, (Student's *t* test).**

Figure S3.

OmpA dependent invasion and intracellular proliferation of *Salmonella* inside the epithelial cell.

(A) Caco-2 cells and HeLa cells were infected with log phase culture of STM- (WT), *ΔompA*, *ΔompA*: pQE60-*ompA*, & *ΔompA*: pQE60 respectively at MOI 10. 2 hours post-infection the cells were lysed and plated. The CFU at 2 hours was normalized with pre-inoculum to calculate the percent invasion in epithelial cells, (n=3, N=3). (B) HeLa cells were infected with log phase culture of STM- (WT), *ΔompA*, *ΔompA*: pQE60-*ompA*, & *ΔompA*: pQE60 respectively at MOI 50. Cells were fixed at 25 minutes post-infection with PFA. Externally attached bacteria were probed with anti-*Salmonella* antibody without saponin. 20 microscopic fields were analyzed to calculate the no. of adherent bacteria/ total no. of cells per field, (n=20, N=3). Scale bar = 20µm. (C) Caco-2 and HeLa cells were infected with log phase culture of STM- (WT), *ΔompA*, *ΔompA*: pQE60-*ompA*, & *ΔompA*: pQE60 respectively at MOI 10. 16- and 2-hours post-infection the cells were lysed and plated. The CFU at 16 hours were normalized with the CFU at 2 hours to calculate the fold proliferation of bacteria in epithelial cells, (n=3, N=3). (D) Caco-2 cells were infected with STM- (WT): RFP, *ΔompA*: RFP, and *ΔompA*: pQE60-*ompA* at MOI 20. PFA fixed wild-type bacteria was used for infection at MOI 25. Cells were fixed at 16 hours post-infection & LAMP-1 was labeled with anti-human LAMP-1 antibody. The complemented strain and PFA fixed dead bacteria were tracked with an anti-*Salmonella* antibody. The quantification of LAMP-1 recruitment on bacteria in Caco-2 cells has been represented in form of a graph. Percent colocalization was determined after analyzing 50 different microscopic fields from three independent experiments. Scale bar = 5µm, (n=50, N=3). (E) Chloroquine resistance assay of Caco-2 cells infected with STM- (WT), *ΔompA*, *ΔompA*: pQE60-*ompA* strains, (n=3, N=2).

(P)* *< 0.05, *(P)* **< 0.005, *(P)* ***< 0.0005, *(P)* *< 0.0001, ns= non-significant, (Student's *t*-test).**

Figure S4.

STM *ΔompA* comes out into the cytoplasm of the macrophage after quitting the vacuole.

(A) Verification of the sub-cellular niche of STM- (WT) and *ΔompA* in macrophage by flow cytometry. RAW264.7 cells were infected with STM- (WT) and *ΔompA* labeled with pH rhodo red dye at MOI 50. Uninfected RAW264.7 cells were used as unstained control. 12 hours post-infection the cells were harvested and subjected to analysis by flow cytometry. The dot plots (of SSC-A vs pH rhodo red) and histograms from one experiment out of three independently carried out experiments have been represented here. The median fluorescence intensity of pH rhodo red for both STM- (WT) and *ΔompA* strains has been represented in form of a graph. The representative image has been chosen from three independently carried out experiments. (n=5, N=3). (B-E) RAW264.7 cells were infected with STM (WT)-: RFP, *ΔompA*: RFP, at MOI 20. Cells were fixed at 16 hours post-infection, *Salmonella* SPI-2 encoded translocon proteins SseC and SseD were labeled with anti- *Salmonella* SseC/ SseD antibody. (F), (H) The quantification of SseC and SseD recruitment on bacteria in RAW 264.7 cells respectively. Percent colocalization was determined after analyzing 50 different microscopic fields from three independent experiments. Scale bar = 5μm, (n=50, N=3). (G), (I) The transcript level expression of *sseC* and *sseD* in STM (WT) and *ΔompA* growing intracellularly in RAW264.7 cells 12 hours post-infection, (n=3, N=3).

(P)* **< 0.005, *(P)* ***< 0.0005, *(P)* *< 0.0001, ns= non-significant, (Student's t test).**

Figure S5.

OmpA doesn't have a significant role in building up *in vitro* and *in vivo* protection of *Salmonella* against oxidative stress.

(A) Estimation of the level of intracellular reactive oxygen species (ROS) in RAW 264.7 cells infected with STM- (WT), *ΔompA*, and *ΔompA*: pQE60-*ompA* at MOI 10, 16 hours post-

infection using DCFDA [10 µM] by flow cytometry. Unstained and uninfected RAW264.7 cells have also been used as controls. Both dot plots (SSC-A vs DCFDA) and histograms (Count vs DCFDA) have been represented. (B) The percent population of DACFDA positive RAW264.7 cells, (n=4, N=3). (C) Estimation of extracellular ROS from the culture supernatant of RAW264.7 cells infected with STM- (WT), *ΔompA*, *ΔompA*: pQE60-*ompA*, *ΔompA*: pQE60, & PFA fixed dead bacteria respectively at MOI 10. 2 hours post-infection the cells were supplemented with phenol red solution having horse radish peroxidase. 16 hours post-infection the culture supernatants were collected, and the OD was measured at 610 nm, (n=3, N=2). (D) Checking the *in vitro* sensitivity of STM- (WT) and *ΔompA* in presence of H_2O_2 by serial dilution, plating, and CFU calculation and resazurin test. 10^8 CFU of overnight grown stationary phase culture of STM (WT) and *ΔompA* were inoculated in PBS with varying concentrations of H_2O_2. 12 hours post-inoculation the supernatants were collected for plating on SS agar to determine the $\log_{10}$[CFU/mL] (N=3), and resazurin test to determine percent viability. (n=3, N=3). (E) Checking the *in vitro* sensitivity of STM– (WT) and *ΔompA* in presence of acidified nitrite by serial dilution, plating, and CFU calculation and resazurin test. 10^8 CFU of overnight grown stationary phase culture of STM (WT) and *ΔompA* were inoculated in PBS (pH=5.4) with varying concentrations of $NaNO_2$. 12 hours post-inoculation the supernatants were collected for plating on SS agar to determine the $\log_{10}$[CFU/mL], (N=3) and resazurin test to determine percent viability. (n=3, N=3). (F) Checking the *in vitro* sensitivity of STM– (WT) and *ΔompA* in presence of $NaNO_2$ and H_2O_2 combined, by serial dilution, plating, and CFU calculation and resazurin test. 10^8 CFU of overnight grown stationary phase culture of STM (WT) and *ΔompA* were inoculated in PBS (pH=5.4) with varying concentrations of $NaNO_2$ and H_2O_2. 12 hours post-inoculation the supernatants were collected for plating on SS agar to determine the $\log_{10}$[CFU/mL] (N=3), and resazurin test to determine percent viability, (n=3, N=3).

(P)* *< 0.05, *(P)* **< 0.005, *(P)* ***< 0.0005, *(P)* *< 0.0001, ns= non-significant, (2way ANOVA), (Student's *t* test).**

Figure S6.

Generation and confirmation of *ompA ompC, ompA ompD*, *ompA ompF* double knockouts in STM *ΔompA* and *ompC*, *ompD*, *ompF* single knockouts in STM (WT).

(A-C) To obtain *ompA ompC, ompA ompD*, *ompA ompF* double knockout strains, chloramphenicol resistant gene cassettes (size- 1.1 kb) having a flanking sequence homologous to *ompC, ompD, ompF* respectively, were introduced into STM *ΔompA* harboring pKD46 plasmid by electroporation. Confirmation of (A) *ΔompA ΔompC*, (B) *ΔompA ΔompD,* (C) *ΔompA ΔompF* using respective confirmatory primers. (D-F) To obtain *ompC*, *ompD*, *ompF* single knockout strains chloramphenicol resistant gene cassette (size- 1.1 kb, having a flanking sequence homologous to *ompC, ompD,* and *ompF*) and kanamycin-resistant gene cassette (size- 1.6 kb having a flanking sequence homologous to *ompD*) were introduced into STM (WT) harboring pKD46 plasmid. Confirmation of (D) *ompC*, (E) *ompD*, (F) *ompF* using respective confirmatory primers.

Figure S7.

Unlike *ompA*, other outer membrane porins (*ompC, ompD, ompF*) don't have any significant role in the protection of *Salmonella* against intracellular and extracellular nitrosative stress.

(A) RAW264.7 cells were infected with STM- (WT), *ΔompA*, *ΔompC*, *ΔompD*, and *ΔompF* at MOI 20. Cells were fixed at 16 hours post-infection, followed by labeled with anti-*Salmonella* antibody and anti-mouse nitrotyrosine antibody respectively. Quantification of nitrotyrosine

recruitment on STM- (WT), *ΔompA*, *ΔompC*, *ΔompD*, and *ΔompF* has been represented in form of a graph. Percent colocalization of bacteria with nitrotyrosine has been determined after analyzing more than 60 different microscopic fields from two independent experiments, ($n \geq 60$, N=3). Scale bar = 5μm. (B) Checking the *in vitro* sensitivity of STM– (WT), *ΔompA*, *ΔompC*, *ΔompD*, and *ΔompF* in presence of acidified nitrite by serial dilution, plating, and CFU calculation. 10^8 CFU of overnight grown stationary phase culture of STM (WT), *ΔompA, ΔompC, ΔompD,* and *ΔompF* were inoculated in PBS (pH=5.4) with varying concentration of $NaNO_2$. 12 hours post-inoculation the supernatants were collected for plating on SS agar to determine the $\log_{10}$[CFU/mL], (N=3). (C) *In vitro* nitrite uptake assay of STM- (WT), *ΔompA*, *ΔompC, ΔompD, ΔompF* & PFA fixed dead bacteria. 10^8 CFU of overnight grown stationary phase culture of all the strains were inoculated in MOPS- NaOH buffer (pH= 8.5) with an initial nitrite concentration of 50 μM. The remaining nitrite concentration of the media was determined by Griess assay at 0, 1, 2, 3, 4, 5, and 6 hours post-inoculation, (n=3, N=3).

(P)* *< 0.05, *(P)* **< 0.005, *(P)* ***< 0.0005, *(P)* *< 0.0001, ns= non-significant, (2way ANOVA), (Student's *t* test).**

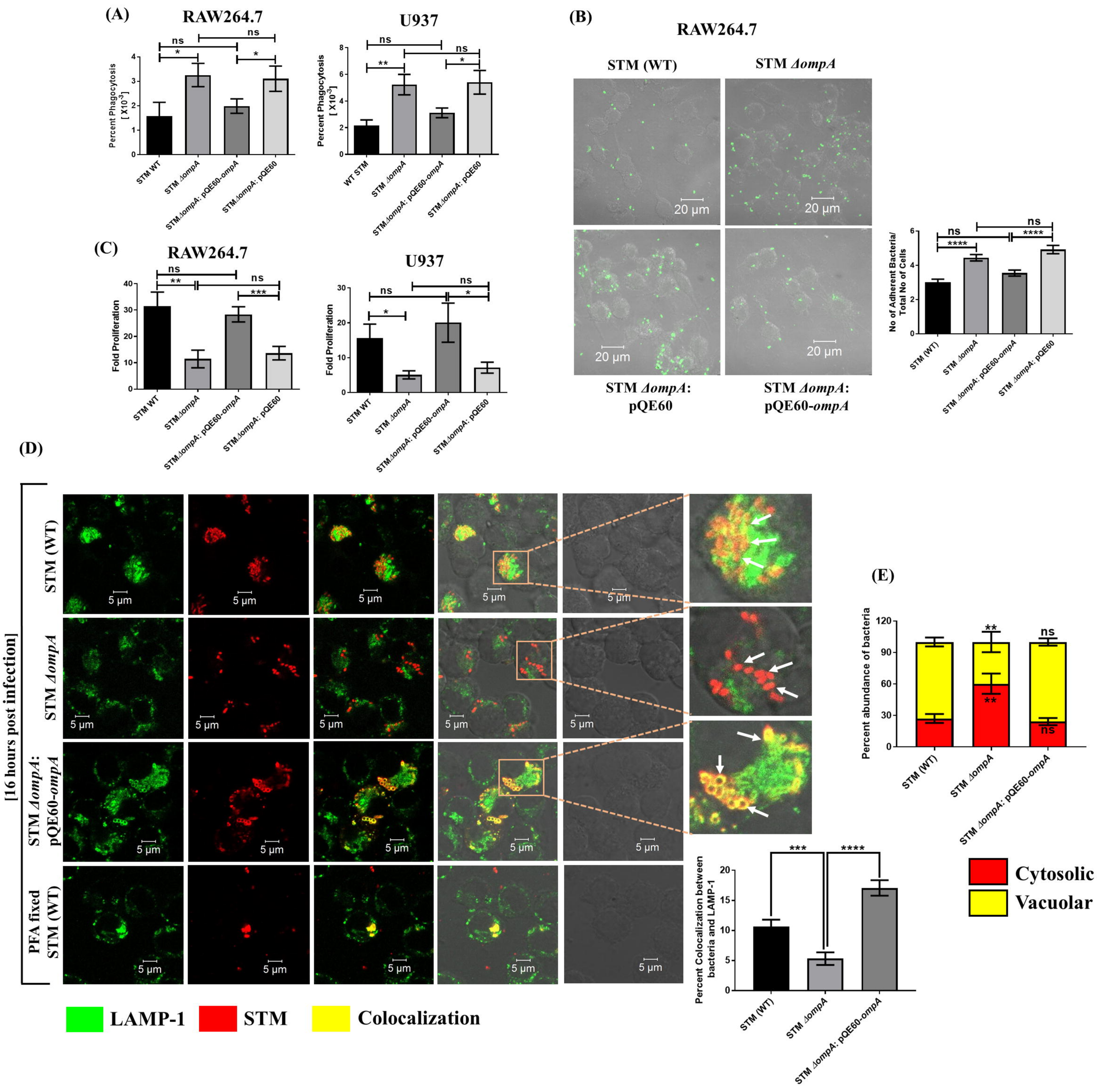
(A)
RAW264.7
U937
Percent Phagocytosis [X10^-3]
STM WT
STM ΔompA
STMΔompA: pQE60-ompA
STMΔompA: pQE60
WT STM
(B)
RAW264.7
STM (WT)
STM ΔompA
STM ΔompA: pQE60
STM ΔompA: pQE60-ompA
20 µm
No of Adherent Bacteria/ Total No of Cells
(C)
RAW264.7
U937
Fold Proliferation
(D)
[16 hours post infection]
STM (WT)
STM ΔompA
STM ΔompA: pQE60-ompA
PFA fixed STM (WT)
5 µm
LAMP-1
STM
Colocalization
Percent Colocalization between bacteria and LAMP-1
(E)
Percent abundance of bacteria
Cytosolic
Vacuolar

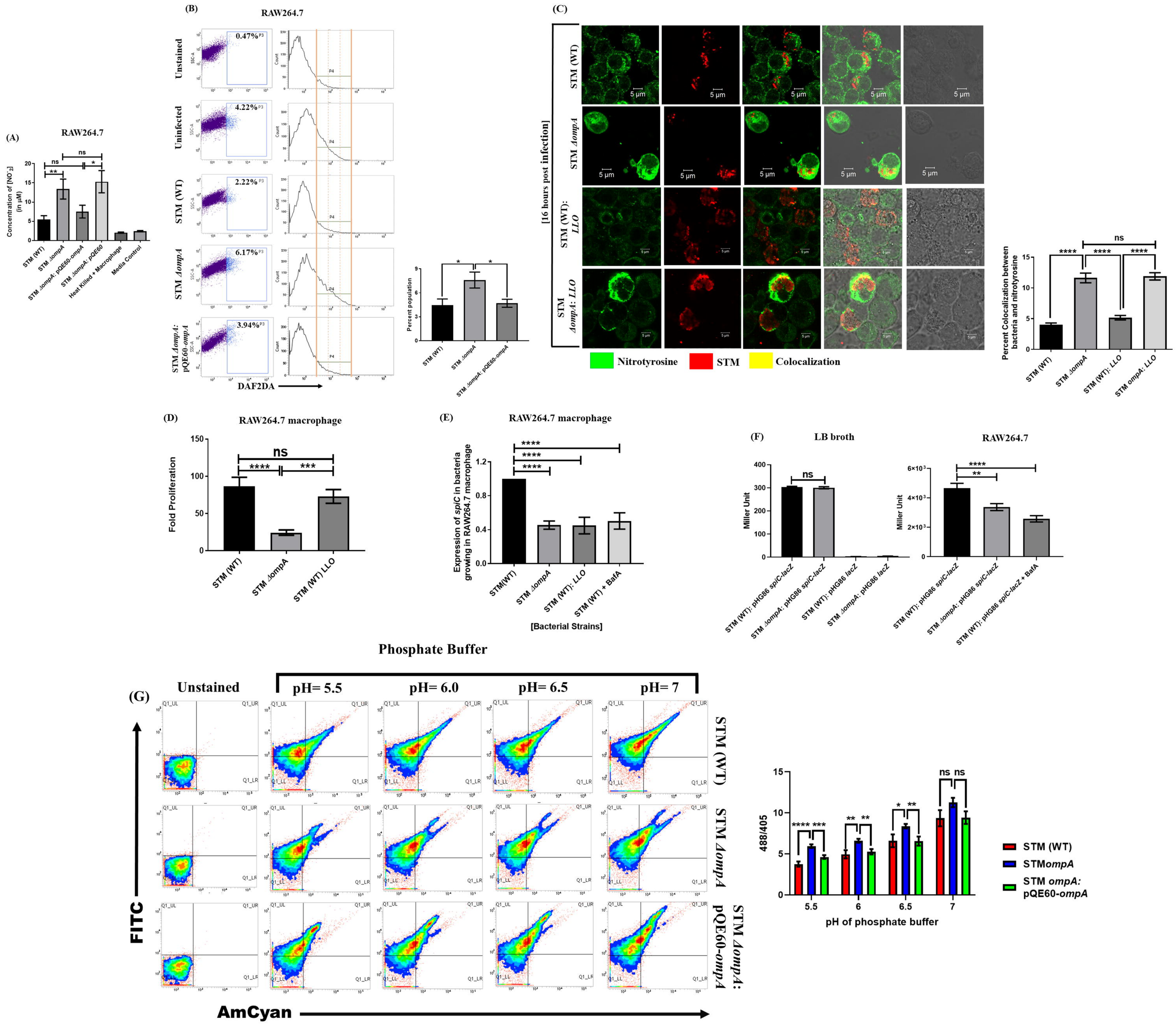
(A)
RAW264.7
Concentration of [NO-2] (in µM)
STM (WT)
STM ΔompA
STM ΔompA: pQE60-ompA
STM ΔompA: pQE60
Heat Killed + Macrophage
Media Control
(B)
RAW264.7
Unstained
Uninfected
STM (WT)
STM ΔompA
STM ΔompA: pQE60-ompA
0.47%
4.22%
2.22%
6.17%
3.94%
DAF2DA
Percent population
(C)
[16 hours post infection]
STM (WT)
STM ΔompA
STM (WT): LLO
STM ΔompA: LLO
Nitrotyrosine
STM
Colocalization
Percent Colocalization between bacteria and nitrotyrosine
(D)
RAW264.7 macrophage
Fold Proliferation
STM (WT)
STM ΔompA
STM (WT) LLO
(E)
RAW264.7 macrophage
Expression of spiC in bacteria growing in RAW264.7 macrophage
STM(WT)
STM ΔompA
STM (WT): LLO
STM (WT) + BafA
[Bacterial Strains]
(F)
LB broth
RAW264.7
Miller Unit
STM (WT): pHG86 spiC-lacZ
STM ΔompA: pHG86 spiC-lacZ
STM (WT): pHG86 lacZ
STM ΔompA: pHG86 lacZ
STM (WT): pHG86 spiC-lacZ + BafA
Phosphate Buffer
(G)
Unstained
pH= 5.5
pH= 6.0
pH= 6.5
pH= 7
STM (WT)
STM ΔompA
STM ΔompA: pQE60-ompA
FITC
AmCyan
488/405
pH of phosphate buffer
STMompA
STM ompA: pQE60-ompA

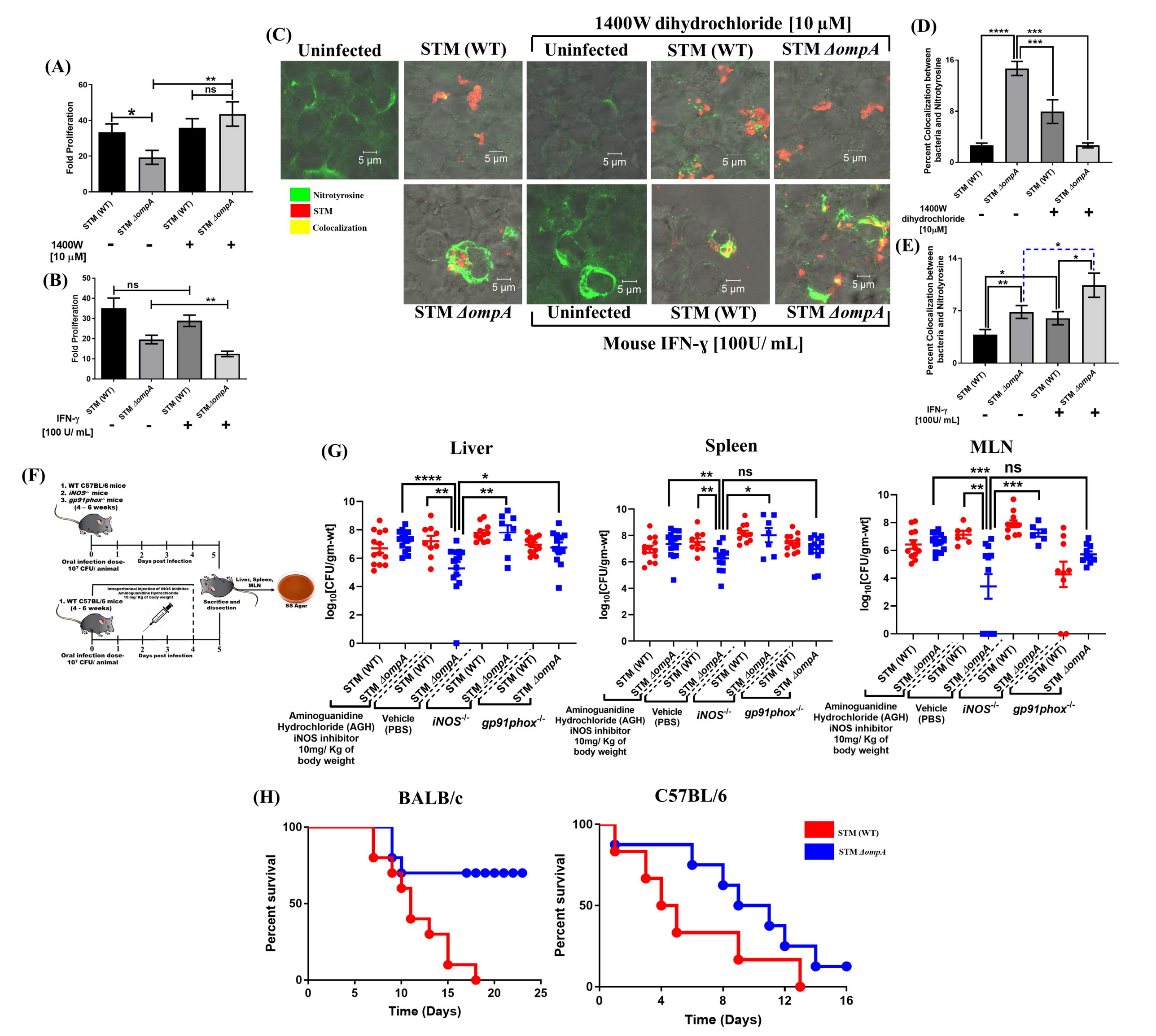
(A)
Fold Proliferation
STM (WT)
STM ΔompA
1400W [10 μM]
(B)
Fold Proliferation
IFN-γ [100 U/ mL]
(C)
Uninfected
STM (WT)
STM ΔompA
1400W dihydrochloride [10 μM]
Nitrotyrosine
STM
Colocalization
5 μm
Mouse IFN-γ [100U/ mL]
(D)
Percent Colocalization between bacteria and Nitrotyrosine
1400W dihydrochloride [10μM]
(E)
IFN-γ [100U/ mL]
(F)
1. WT C57BL/6 mice
2. iNOS-/- mice
3. gp91phox-/- mice
(4 – 6 weeks)
Oral infection dose- 10⁷ CFU/ animal
Days post infection
Intraperitoneal injection of iNOS inhibitor- Aminoguanidine Hydrochloride 10 mg/ Kg of body weight
Sacrifice and dissection
Liver, Spleen, MLN
SS Agar
(G)
Liver
Spleen
MLN
log10[CFU/gm-wt]
Aminoguanidine Hydrochloride (AGH) iNOS inhibitor 10mg/ Kg of body weight
Vehicle (PBS)
iNOS-/-
gp91phox-/-
(H)
BALB/c
C57BL/6
Percent survival
Time (Days)
STM (WT)
STM ΔompA

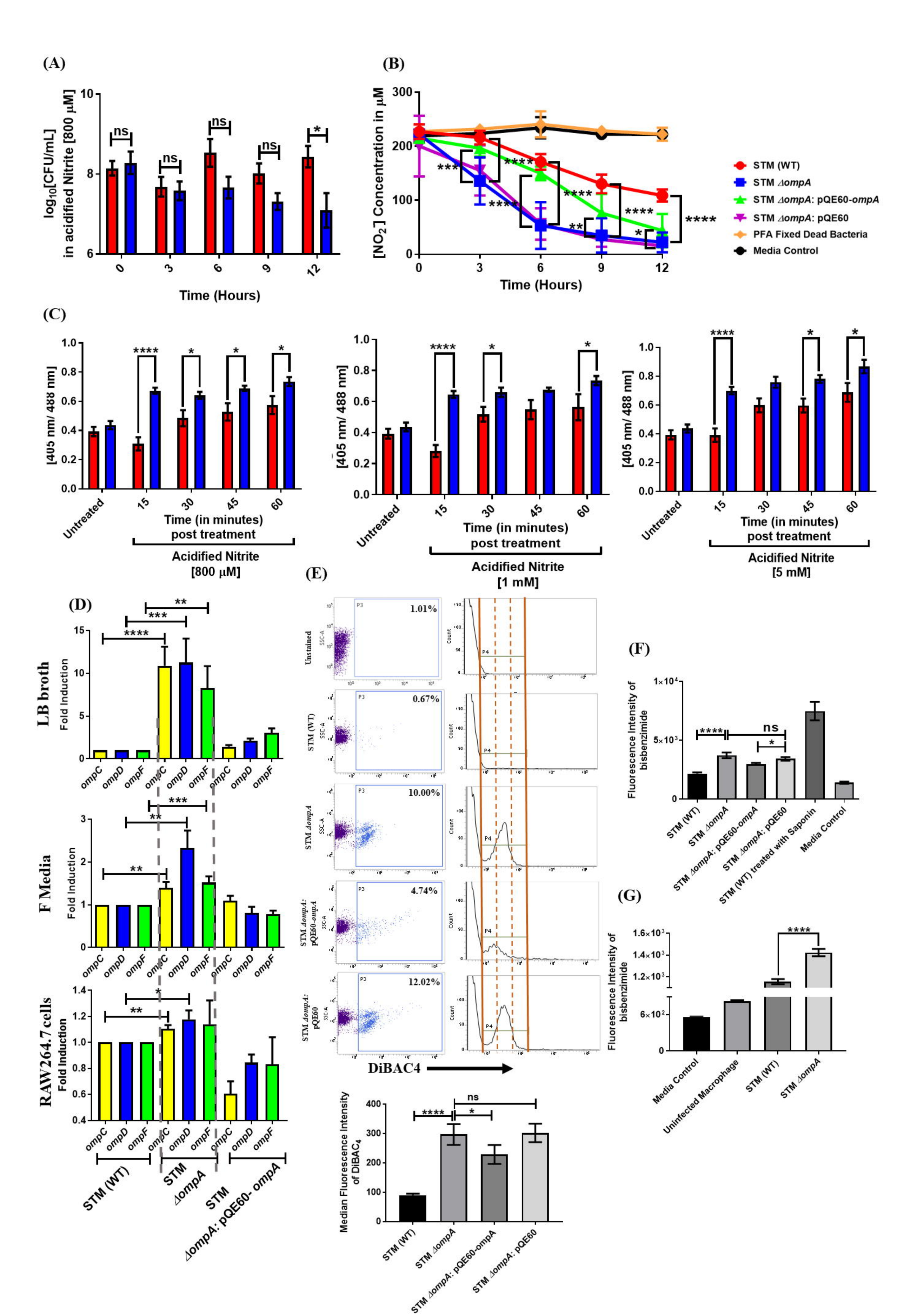
(A)
log10[CFU/mL] in acidified Nitrite [800 μM]
Time (Hours)
(B)
[NO2] Concentration in μM
Time (Hours)
STM (WT)
STM ΔompA
STM ΔompA: pQE60-ompA
STM ΔompA: pQE60
PFA Fixed Dead Bacteria
Media Control
(C)
[405 nm/ 488 nm]
Untreated
Time (in minutes) post treatment
Acidified Nitrite [800 μM]
Acidified Nitrite [1 mM]
Acidified Nitrite [5 mM]
(D)
LB broth
F Media
RAW264.7 cells
Fold Induction
ompC
ompD
ompF
STM (WT)
STM ΔompA
STM ΔompA: pQE60- ompA
(E)
Unstained
STM (WT)
STM ΔompA
STM ΔompA: pQE60-ompA
STM ΔompA: pQE60
1.01%
0.67%
10.00%
4.74%
12.02%
DiBAC4
Median Fluorescence Intensity of DiBAC4
(F)
Fluorescence Intensity of bisbenzimide
STM (WT)
STM ΔompA
STM ΔompA: pQE60-ompA
STM ΔompA: pQE60
STM (WT) treated with Saponin
Media Control
(G)
Fluorescence Intensity of bisbenzimide
Media Control
Uninfected Macrophage
STM (WT)
STM ΔompA

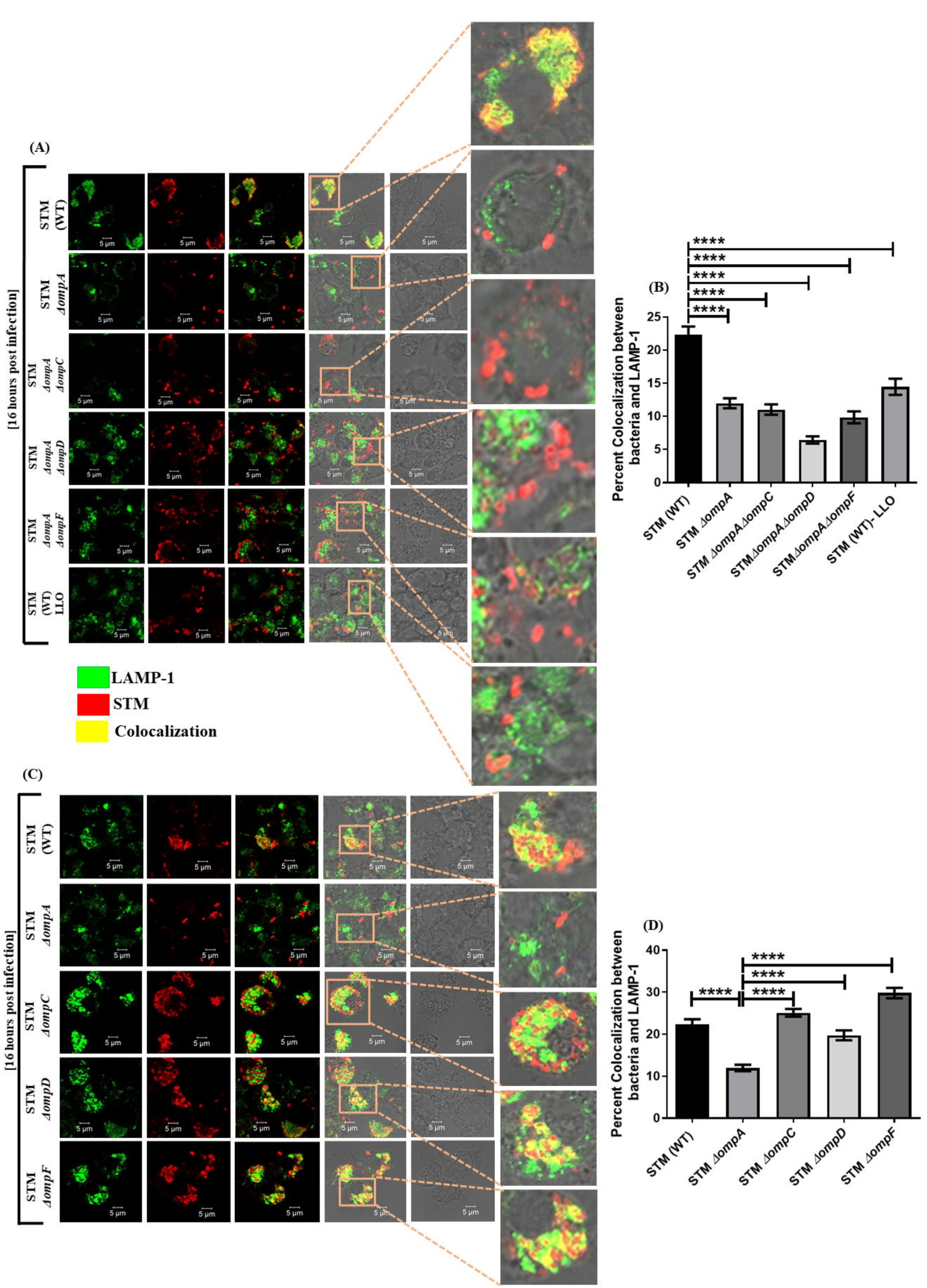
(A)
[16 hours post infection]
STM (WT)
STM ΔompA
STM ΔompA ΔompC
STM ΔompA ΔompD
STM ΔompA ΔompF
STM (WT) LLO
5 µm
LAMP-1
STM
Colocalization
(B)
Percent Colocalization between bacteria and LAMP-1
0
5
10
15
20
25
****
STM (WT)
STM ΔompA
STM ΔompA ΔompC
STM ΔompA ΔompD
STM ΔompA ΔompF
STM (WT)- LLO
(C)
[16 hours post infection]
STM (WT)
STM ΔompA
STM ΔompC
STM ΔompD
STM ΔompF
5 µm
(D)
Percent Colocalization between bacteria and LAMP-1
0
10
20
30
40
****
STM (WT)
STM ΔompA
STM ΔompC
STM ΔompD
STM ΔompF

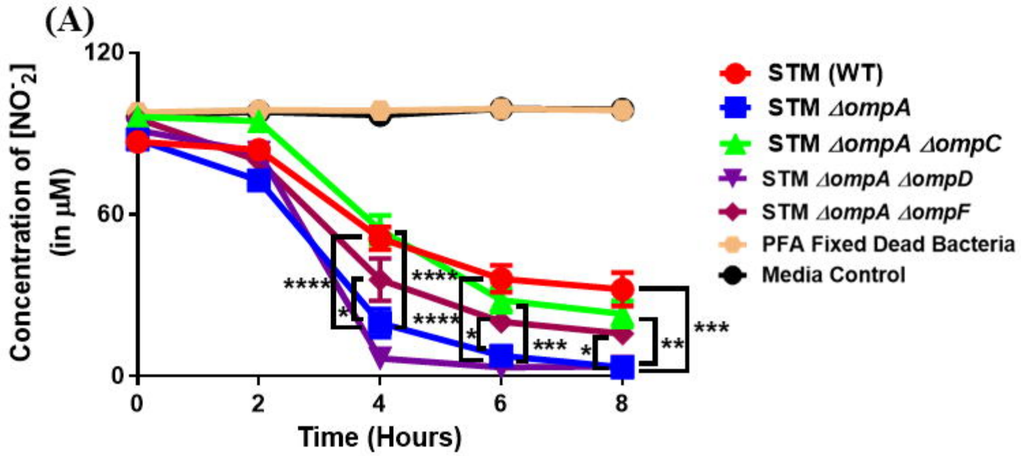

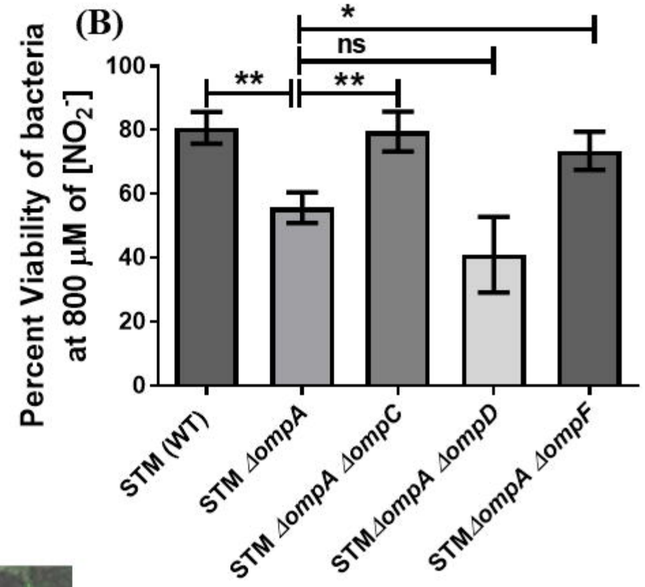

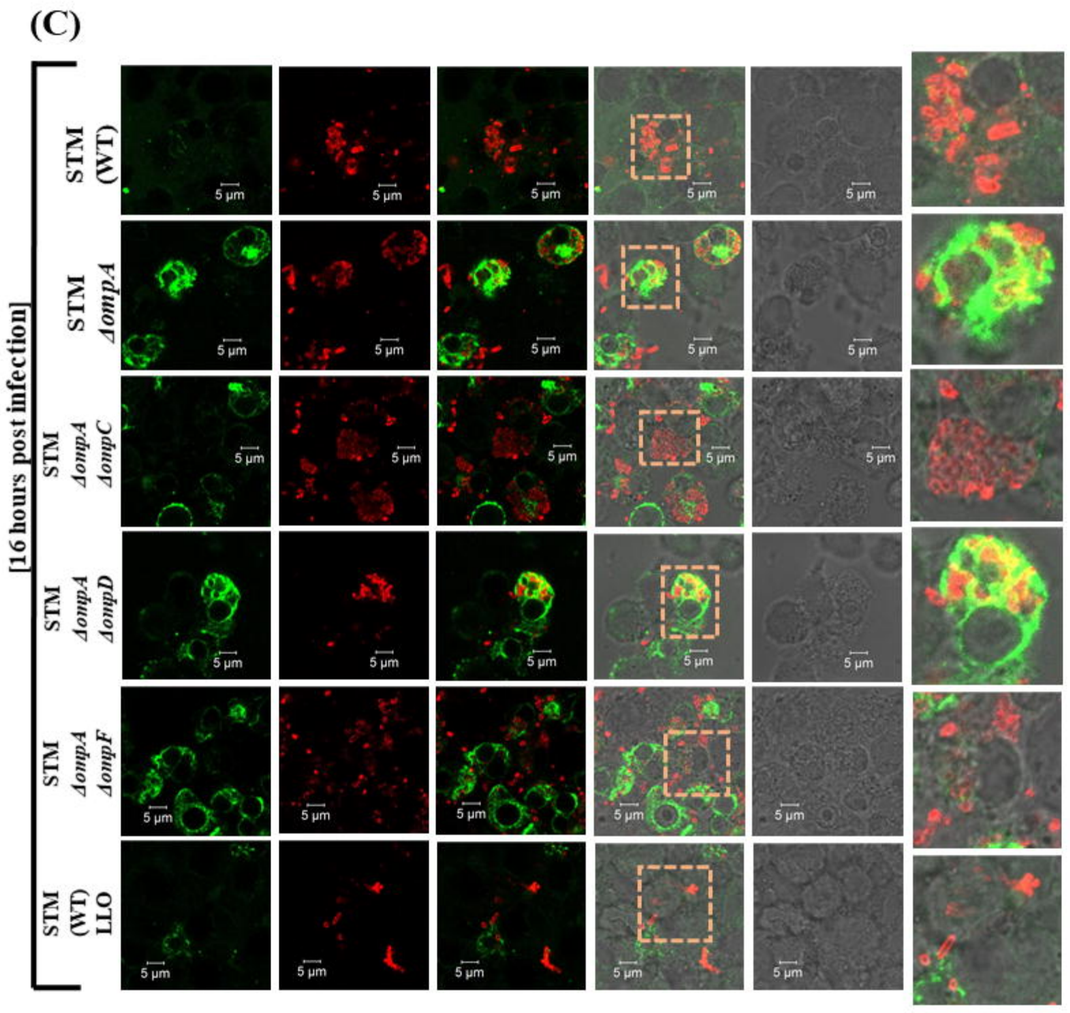

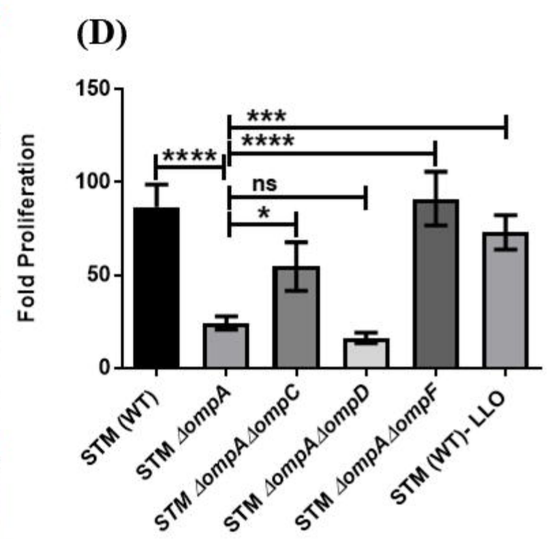

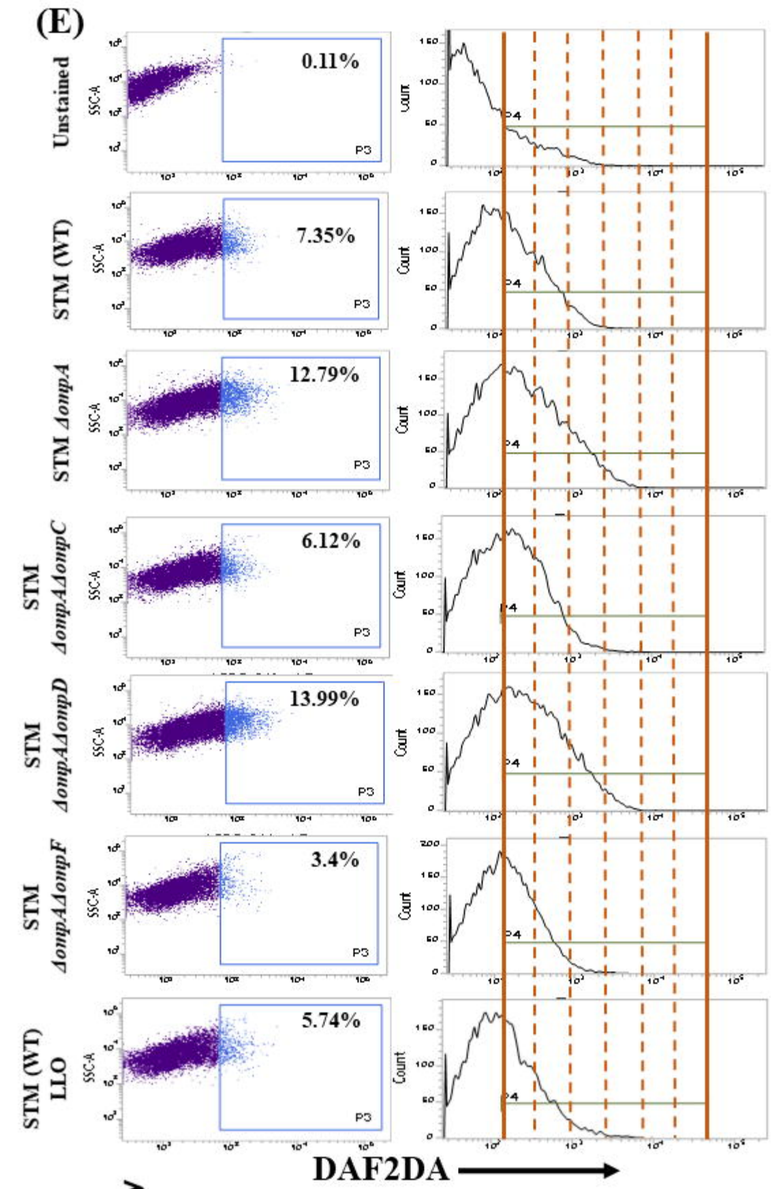

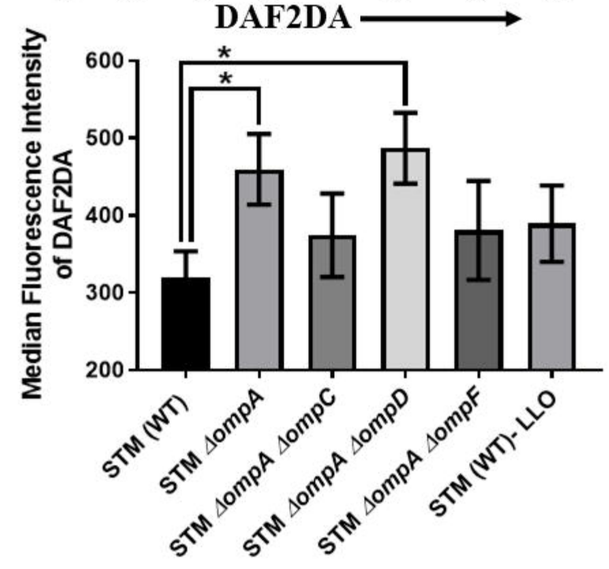

Nitrotyrosine
STM
Colocalization

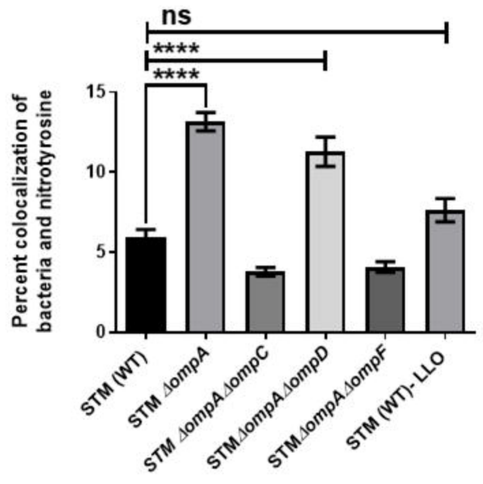

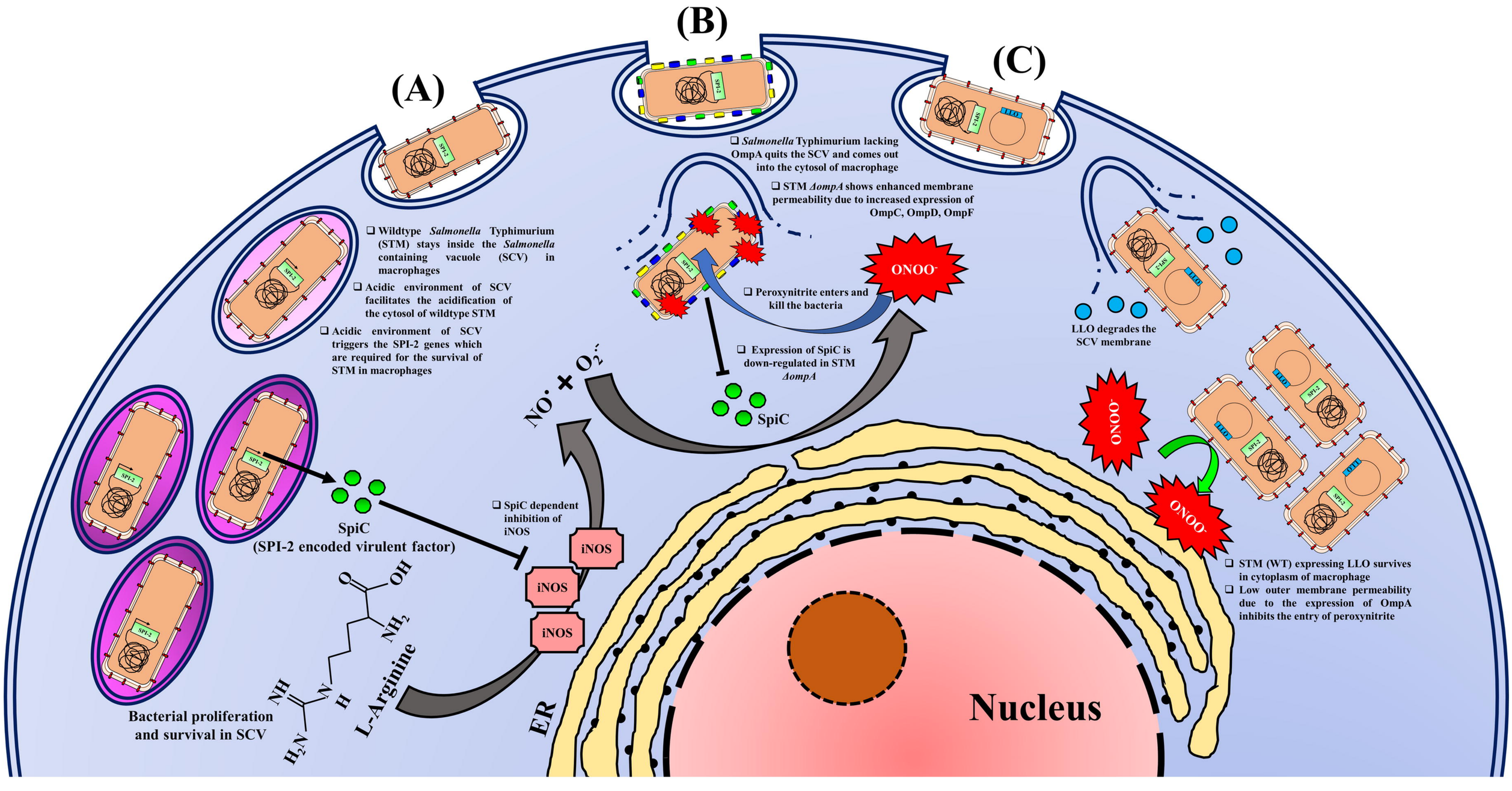
(A)
(B)
(C)
SPI-2
LLO
❑ Wildtype *Salmonella* Typhimurium (STM) stays inside the *Salmonella* containing vacuole (SCV) in macrophages
❑ Acidic environment of SCV facilitates the acidification of the cytosol of wildtype STM
❑ Acidic environment of SCV triggers the SPI-2 genes which are required for the survival of STM in macrophages
❑ *Salmonella* Typhimurium lacking OmpA quits the SCV and comes out into the cytosol of macrophage
❑ STM *ΔompA* shows enhanced membrane permeability due to increased expression of OmpC, OmpD, OmpF
ONOO⁻
❑ Peroxynitrite enters and kill the bacteria
❑ Expression of SpiC is down-regulated in STM *ΔompA*
SpiC
LLO degrades the SCV membrane
NO· + O₂·⁻
SpiC
(SPI-2 encoded virulent factor)
❑ SpiC dependent inhibition of iNOS
iNOS
iNOS
iNOS
L-Arginine
Bacterial proliferation and survival in SCV
ER
Nucleus
ONOO⁻
ONOO⁻
❑ STM (WT) expressing LLO survives in cytoplasm of macrophage
❑ Low outer membrane permeability due to the expression of OmpA inhibits the entry of peroxynitrite